Recent Progress in Cluster Weak Lensing

Cluster Lensing And Supernova survey with Hubble

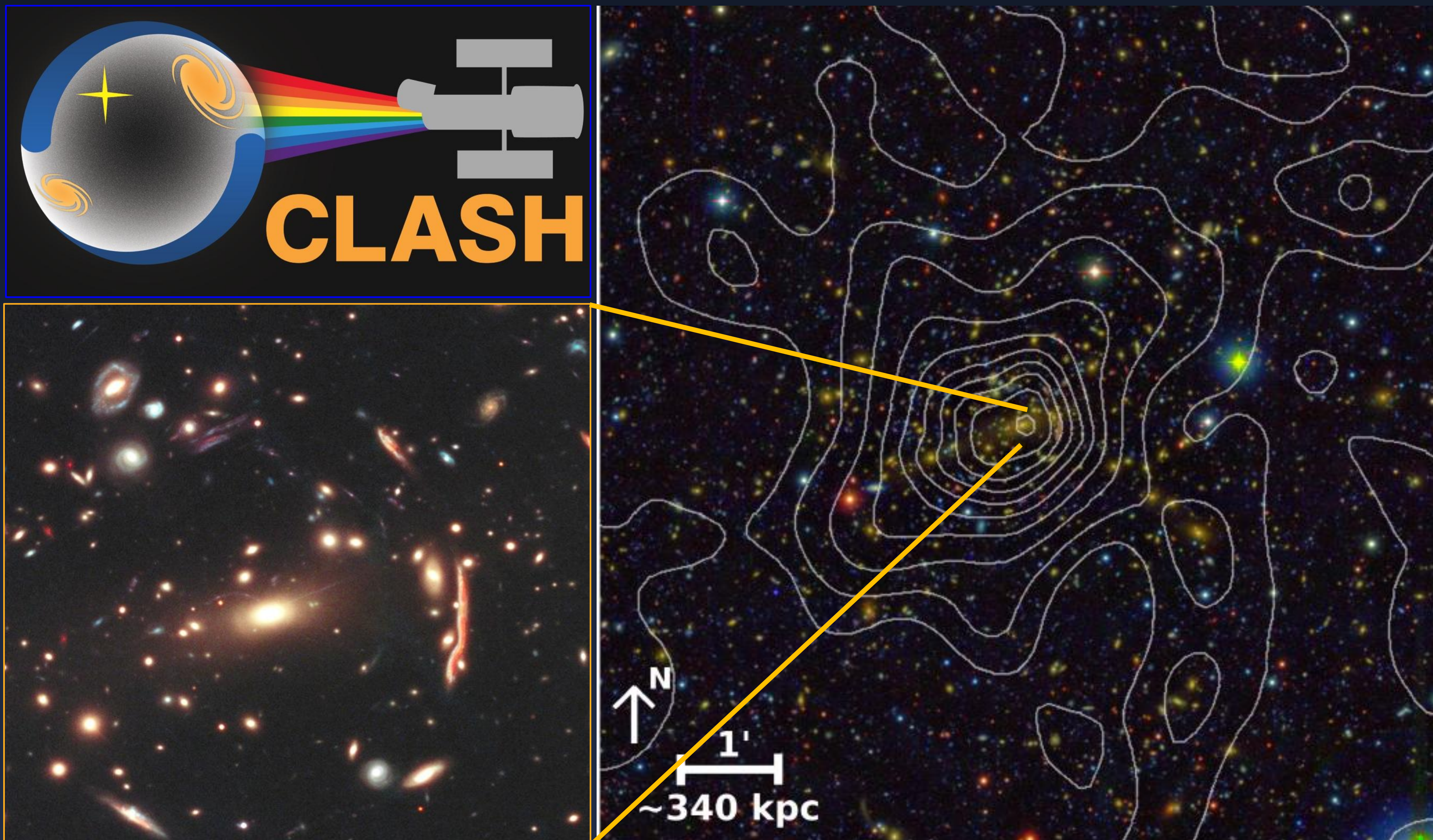

Keiichi Umetsu with T. Broadhurst, E. Medezinski, A. Zitrin, M. Nonino, J. Merten + CLASH

Galaxy Clusters as Cosmological Probe

Cluster counts $n(M,z)$ are exponentially sensitive to ***cosmology***, but also to ***mass calibration***!!!

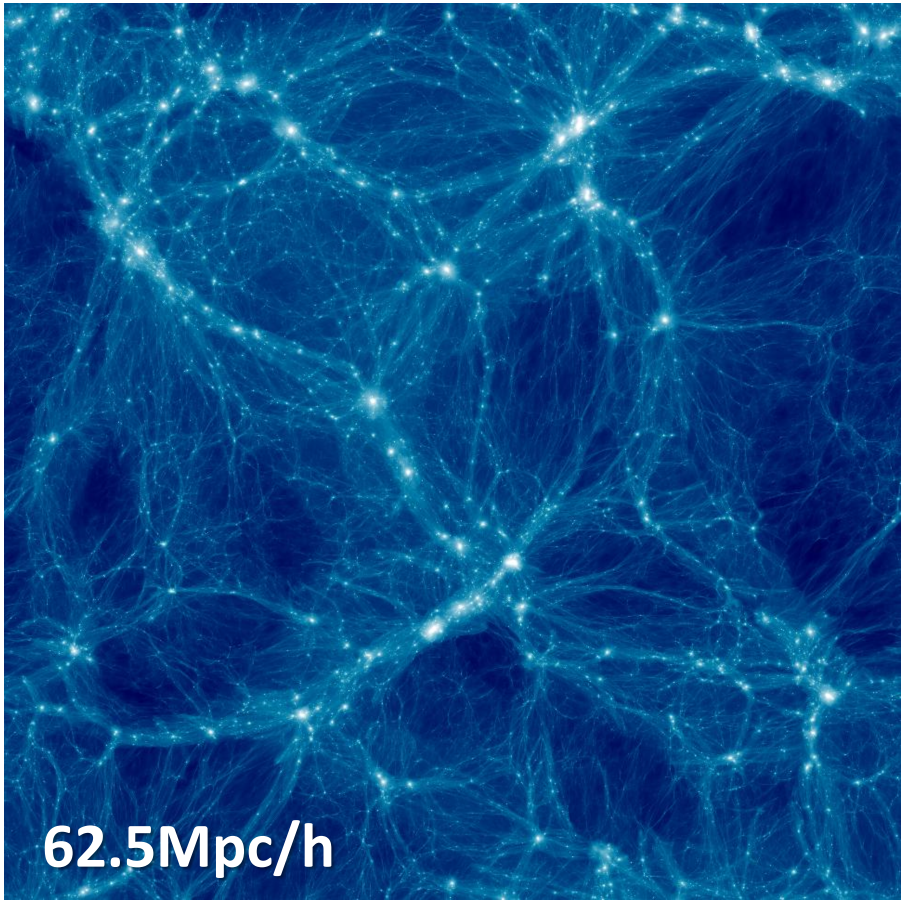

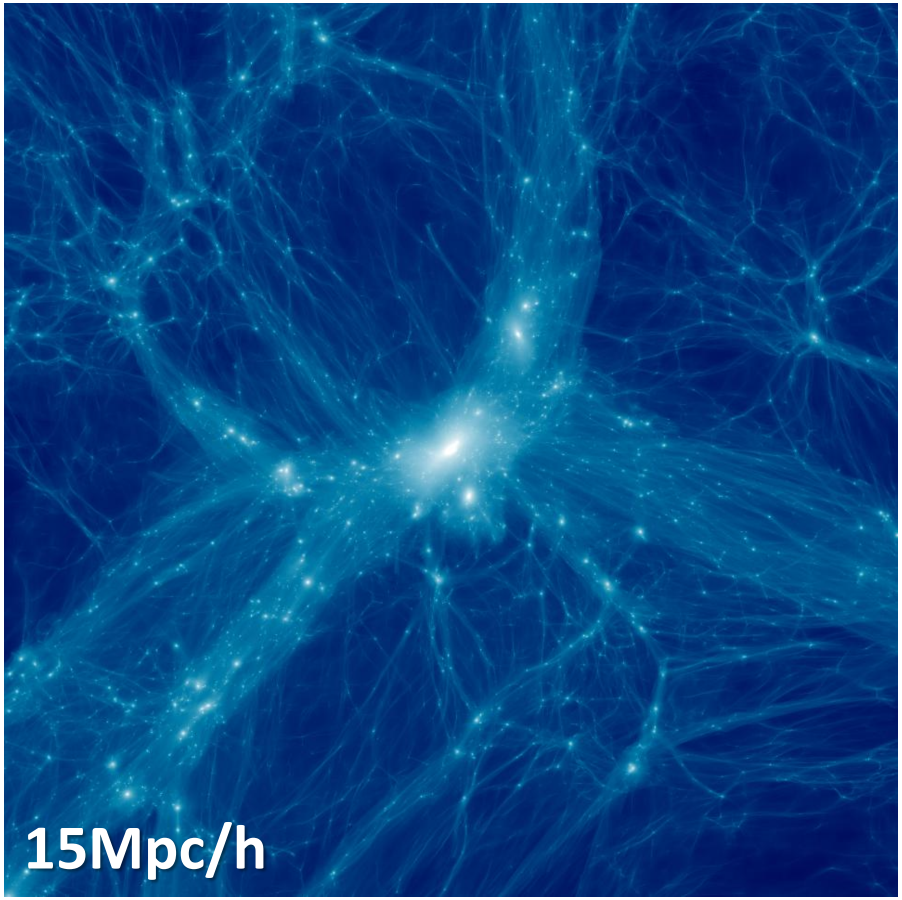

Diemer & Kravtsov 14

Weak Gravitational Lensing

Idlis & Gridneva 1960

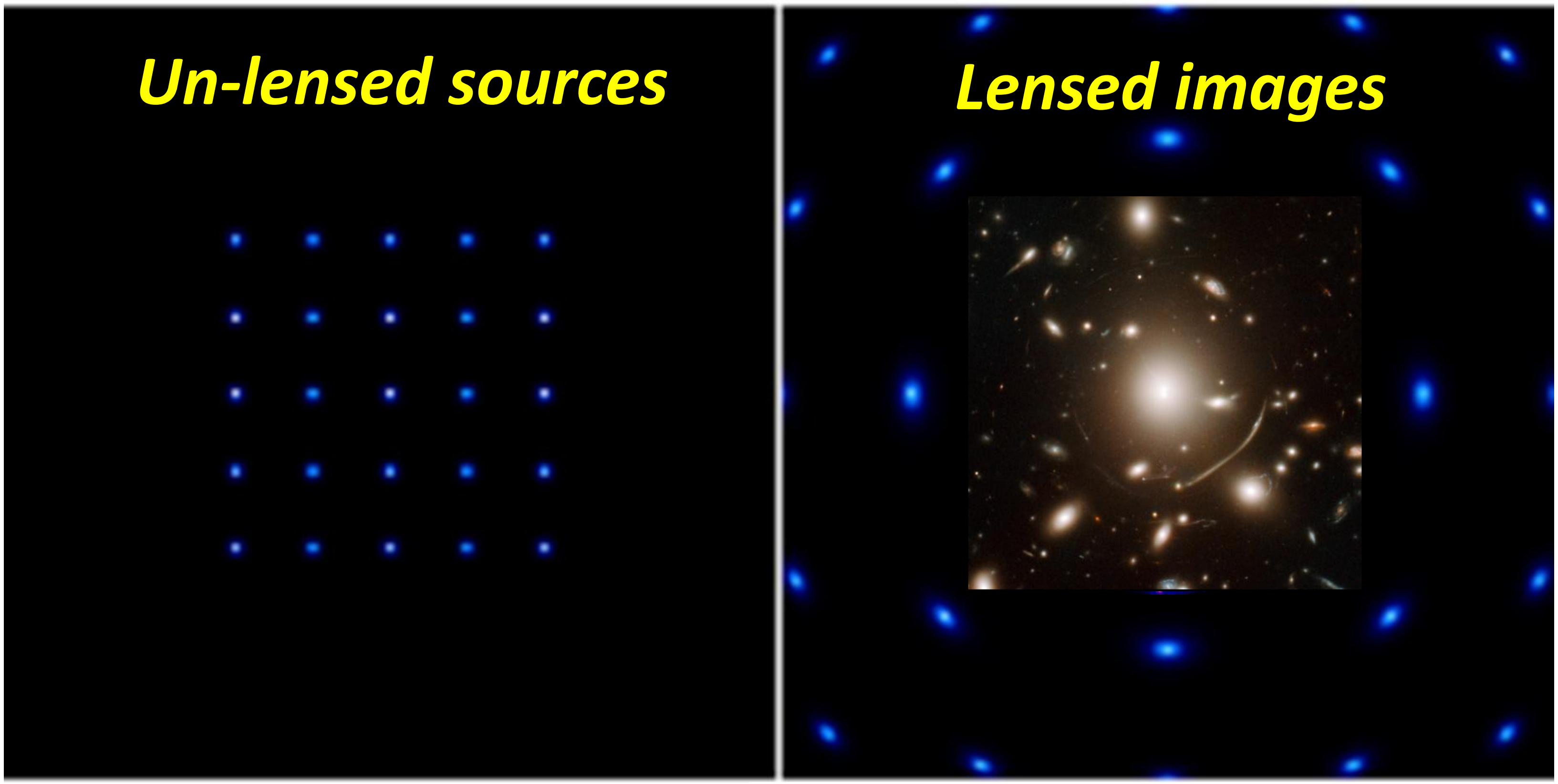

- **Shear** (Kaiser 92, 93, 95)
  - ✓ Shape distortion: $\delta e \sim \gamma$
- **Magnification** (Broadhurst 95)
  - ✓ Flux amplification: μF
  - ✓ Area distortion: $\mu \Delta \Omega$

Sensitive to "modulated" matter density

$$\Sigma_c \gamma_+ = \Delta\Sigma(R) \equiv \Sigma(<R) - \Sigma(R)$$

Sensitive to "total" matter density

$$\mu \approx 1 + 2\kappa; \quad \Sigma_c \kappa = \Sigma(R)$$

Shear fields around Tom's favorite clusters

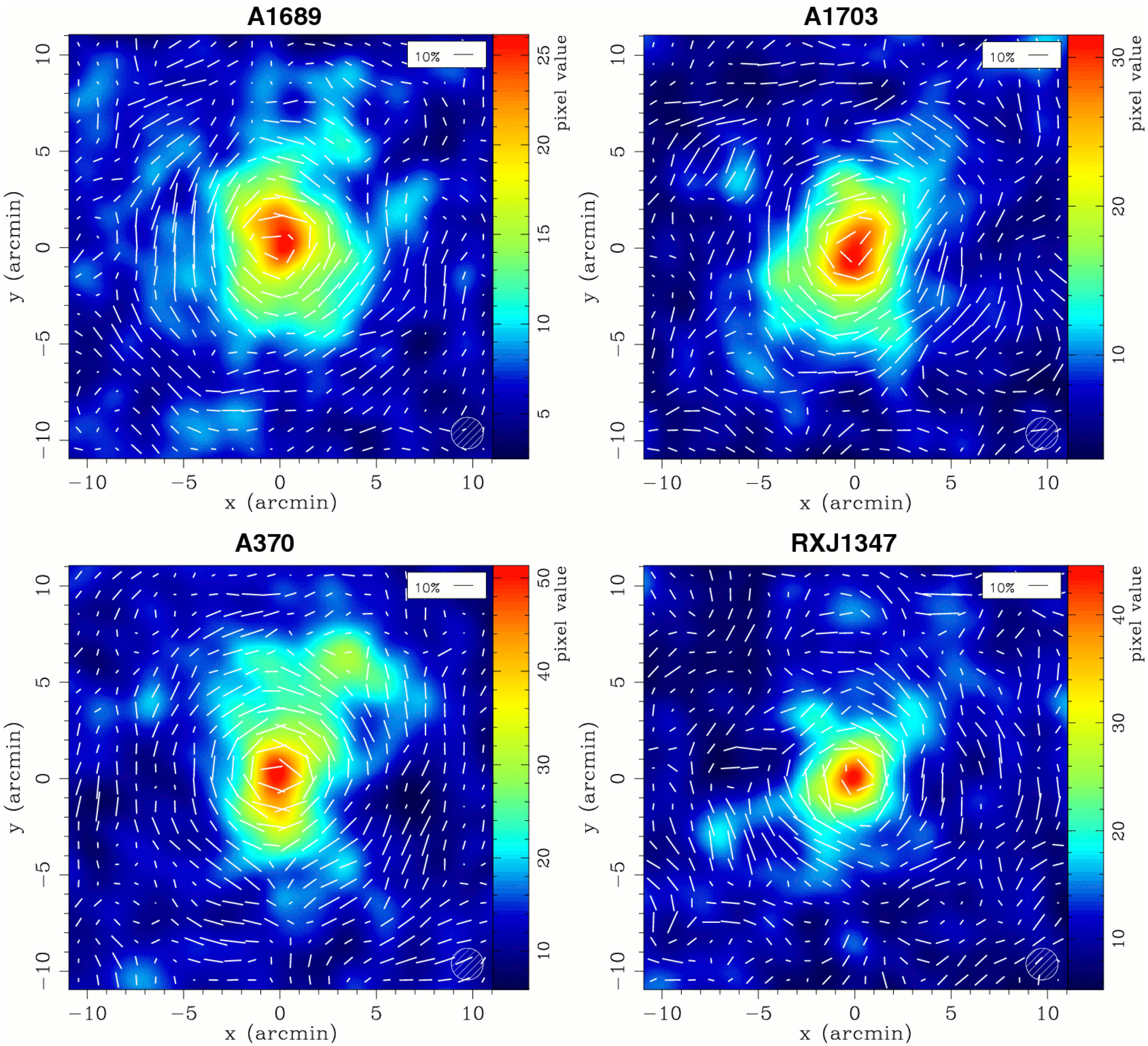

Map: **RS galaxies**

Whiskers: **shear**

Subaru

Suprime-Cam

archival data

Broadhurst,
Umetsu,
Medezinski+08

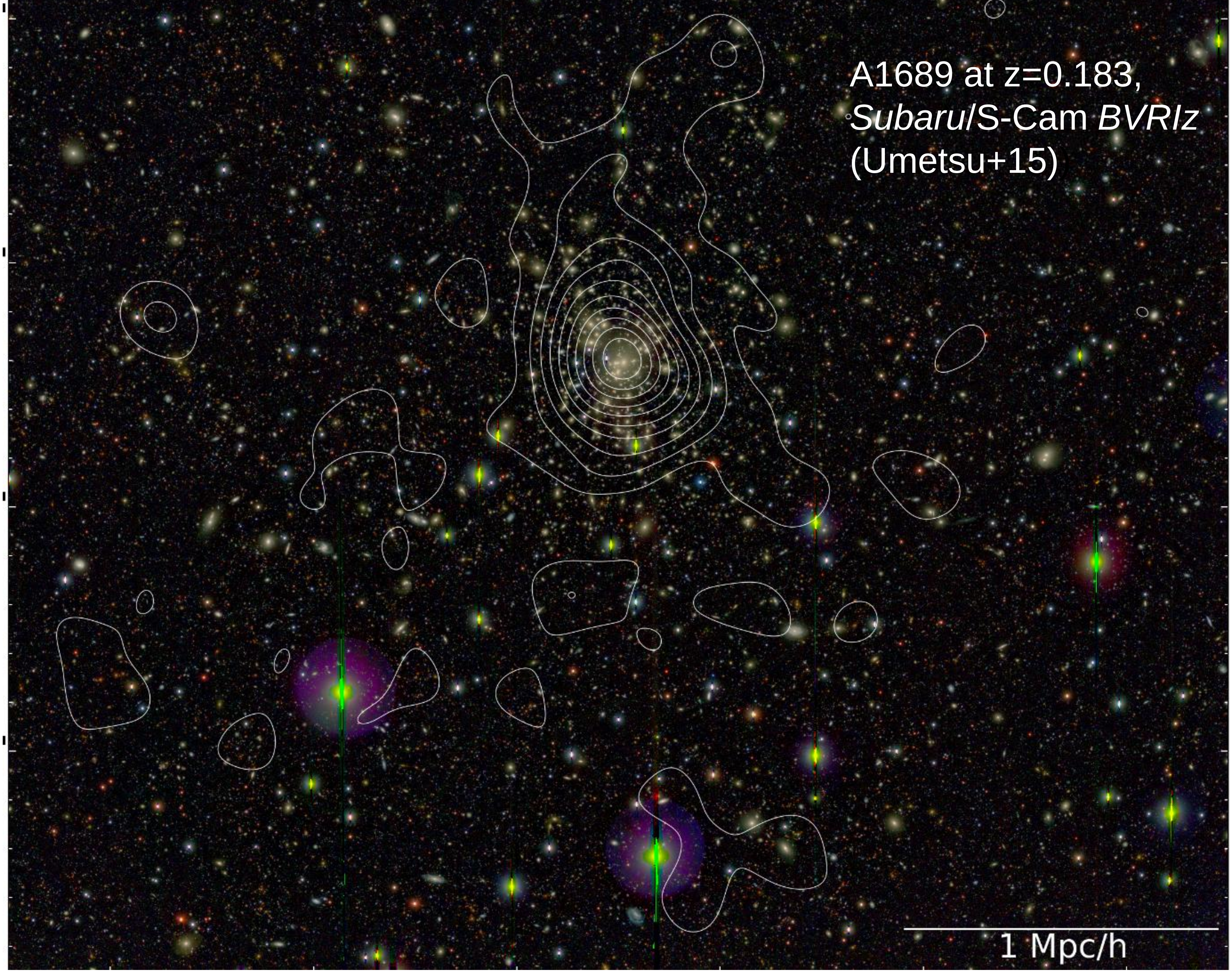
A1689 at z=0.183,
Subaru/S-Cam *BVRIz*
(Umetsu+15)
1 Mpc/h

Shear strength as function of magnitude

$$\gamma \propto \frac{D_{LS}(z)}{D_S(z)}$$

KSB+ (Umetsu+10) pipeline

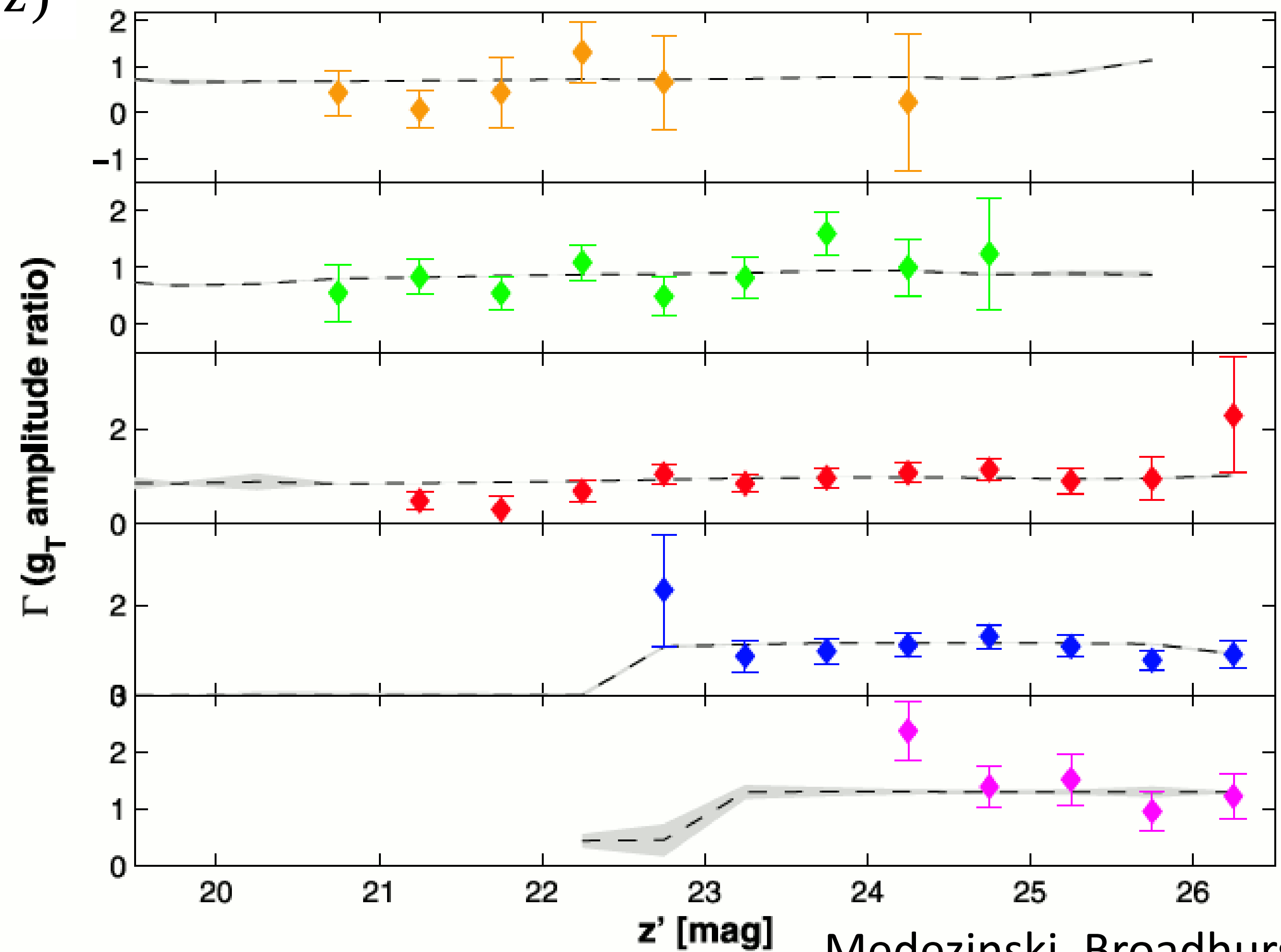

Medezinski, Broadhurst, Umetsu+11

Shear strength as function of z (KSB+)

First detection of WL distance vs. redshift relation!!!

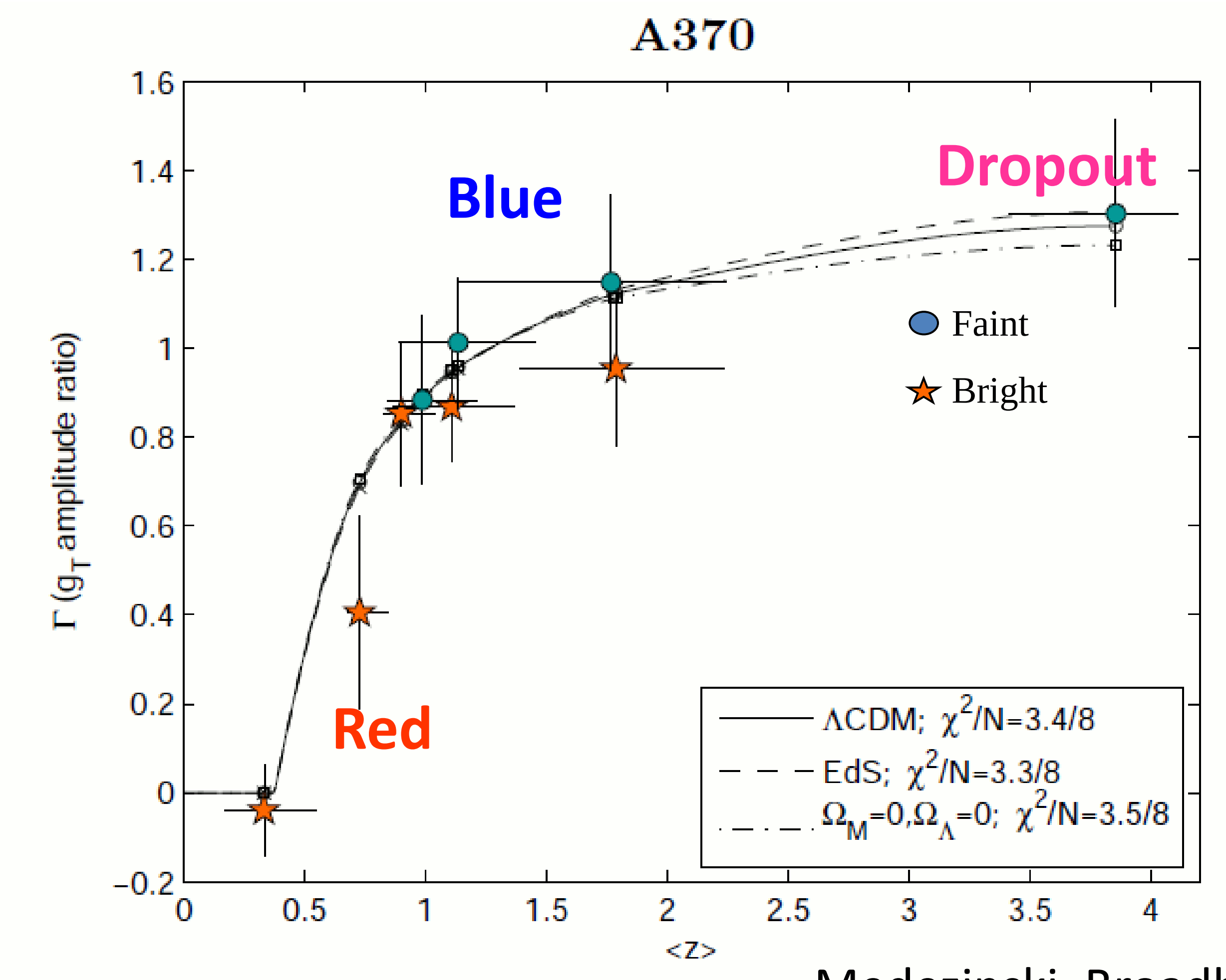

Medezinski, Broadhurst, Umetsu+11

Shear vs. Magnification

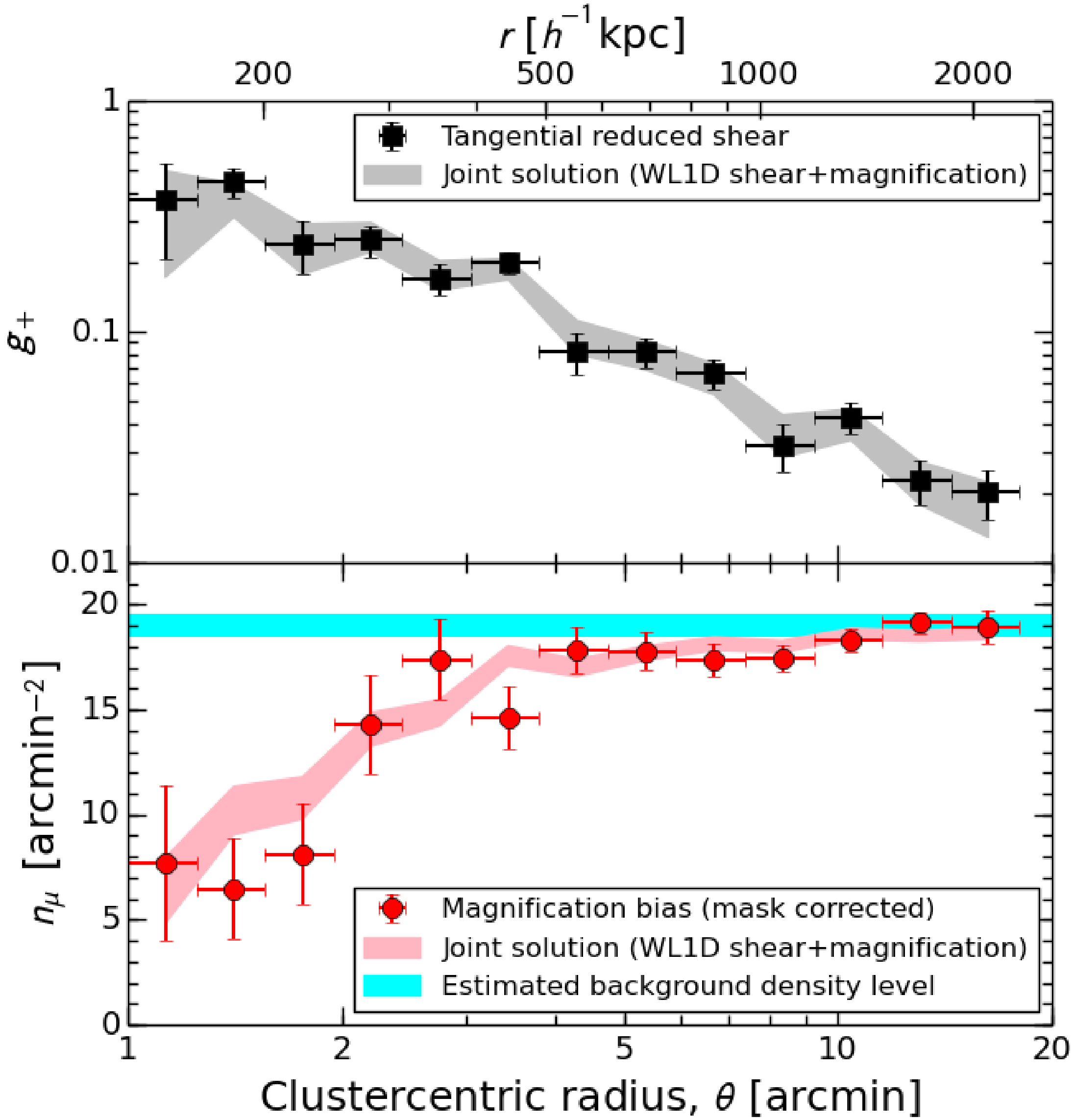

Reduced tangential shear

$$g_+ \approx \gamma_+ = \Delta\Sigma / \Sigma_c$$

Number count depletion due to magnification bias

(Broadhurst, Taylor, & Peacock 95)

$$n_\mu = \bar{n}_\mu \mu^{-1+2.5 s_{\mathrm{eff}}}$$

Subaru *BVRIz* data: A1689
(Umetsu et al. 2015)

Combining Shear and Magnification

Methodology: Umetsu et al. 2011a, ApJ, 729, 127

$$P(\boldsymbol{\kappa}\,|\,\mathrm{WL}) \propto P(\mathrm{WL}\,|\,\boldsymbol{\kappa})P(\boldsymbol{\kappa}) = P(\mathbf{g}_+\,|\,\boldsymbol{\kappa})P(\mathbf{n}_\mu\,|\,\boldsymbol{\kappa})P(\boldsymbol{\kappa})$$

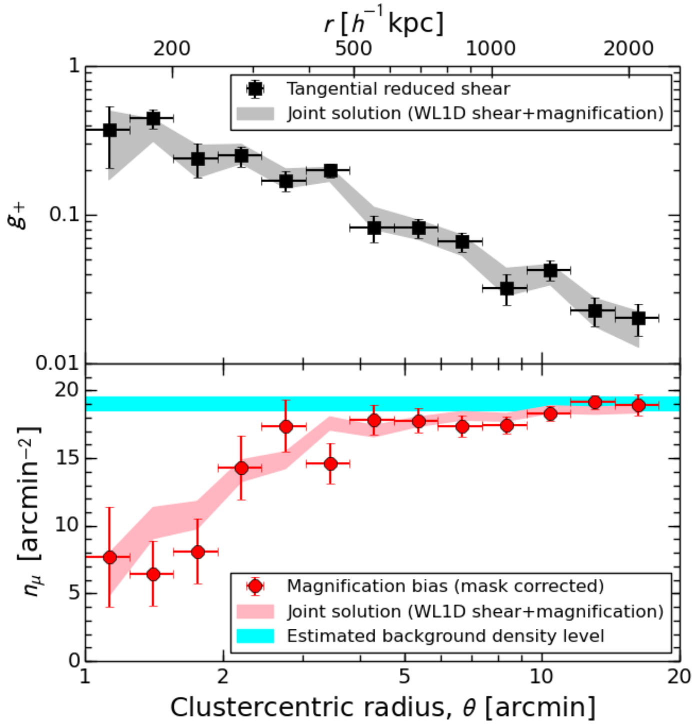

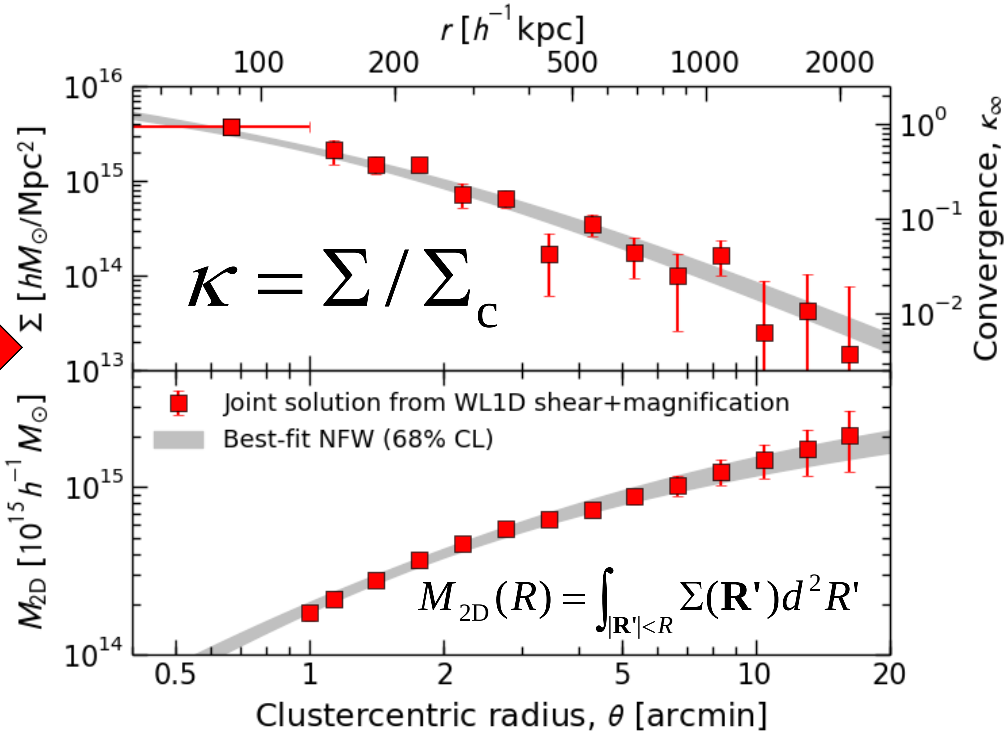

- Mass-sheet degeneracy broken
- Total statistical precision improved by ~20-30%
- Calibration uncertainties marginalized over: $c = \{\langle W\rangle_s, f_{W,s}, \langle W\rangle_\mu, \overline{n}_\mu, s_{\mathrm{eff}}\}.$

Multi-probe Lensing Approach

Combining azimuthally-averaged strong and weak lensing observables

$$M_{\rm 2D}(<R) = \int_{|\mathbf{R}'|<R} \Sigma(\mathbf{R}') d^2R'$$

$$\{M_{{\rm 2D},i}\}_{i=1}^{N_{\rm SL}}, \{\langle g_{+,i}\rangle\}_{i=1}^{N_{\rm WL}}, \{\langle n_{\mu,i}\rangle\}_{i=1}^{N_{\rm WL}}.$$

$$P(\boldsymbol{\kappa}\,|\,{\rm WL,SL}) \propto P({\rm WL,SL}\,|\,\boldsymbol{\kappa})P(\boldsymbol{\kappa}) = P(\mathbf{g}_+\,|\,\boldsymbol{\kappa})P(\mathbf{n}_\mu\,|\,\boldsymbol{\kappa})P(\mathbf{M}_{\rm 2D}\,|\,\boldsymbol{\kappa})P(\boldsymbol{\kappa})$$

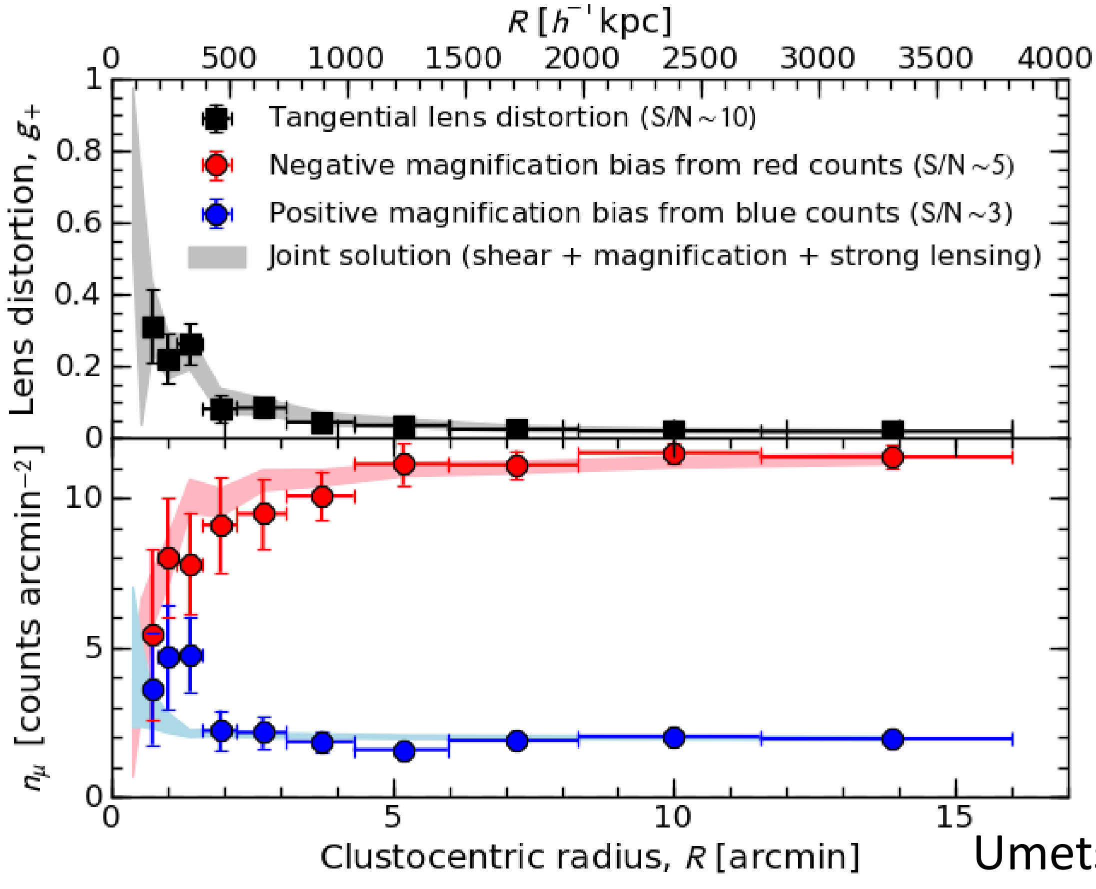

Umetsu 2013, *ApJ*, 769, 13

Multi-probe Lensing Approach

Combining azimuthally-averaged strong and weak lensing observables

$$M_{\rm 2D}(<R) = \int_{|\mathbf{R}'|<R} \Sigma(\mathbf{R}')\, d^2R'$$

$$\{M_{{\rm 2D},i}\}_{i=1}^{N_{\rm SL}}, \{\langle g_{+,i}\rangle\}_{i=1}^{N_{\rm WL}}, \{\langle n_{\mu,i}\rangle\}_{i=1}^{N_{\rm WL}}.$$

$$P(\boldsymbol{\kappa}\,|\,{\rm WL,SL}) \propto P({\rm WL,SL}\,|\,\boldsymbol{\kappa})P(\boldsymbol{\kappa}) = P(\mathbf{g}_+\,|\,\boldsymbol{\kappa})P(\mathbf{n}_\mu\,|\,\boldsymbol{\kappa})P(\mathbf{M}_{\rm 2D}\,|\,\boldsymbol{\kappa})P(\boldsymbol{\kappa})$$

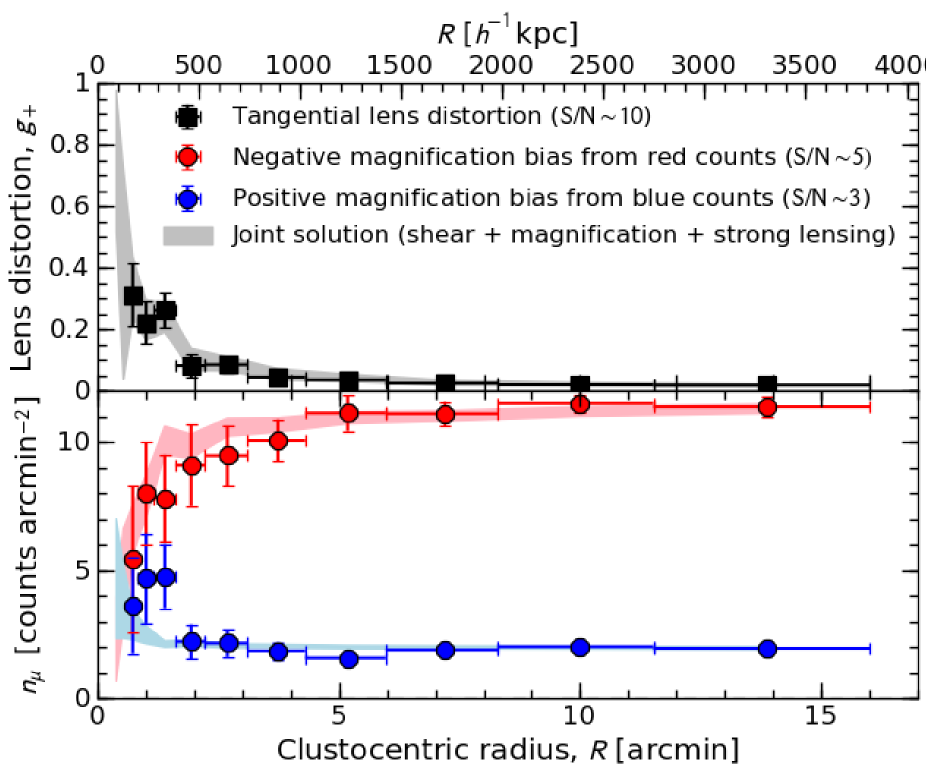

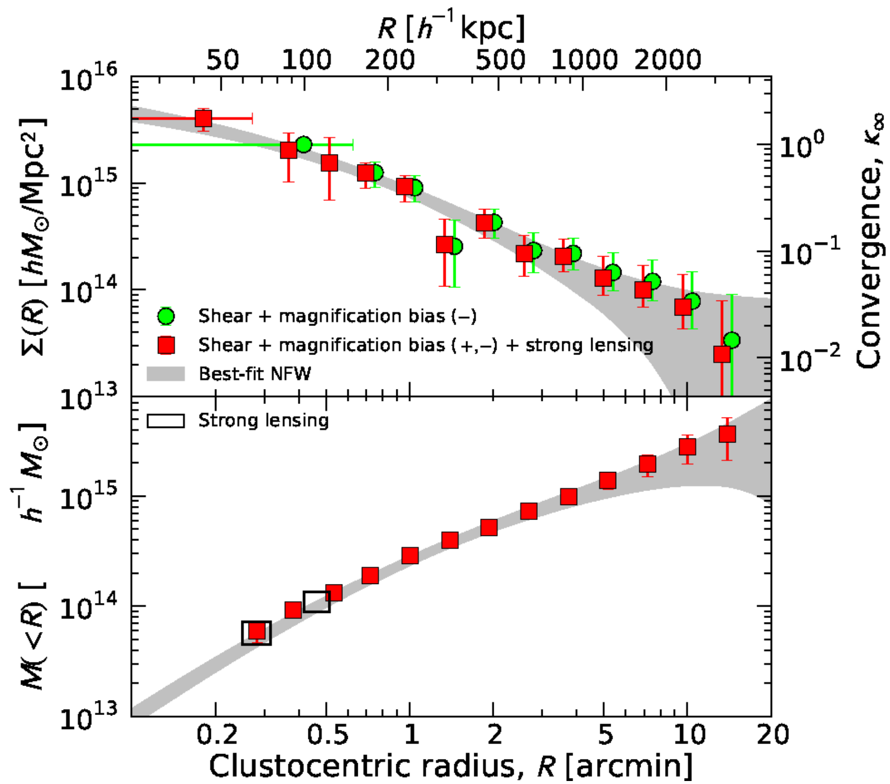

Umetsu 2013, *ApJ*, 769, 13

Cluster Lensing And Supernova survey with Hubble

CLASH

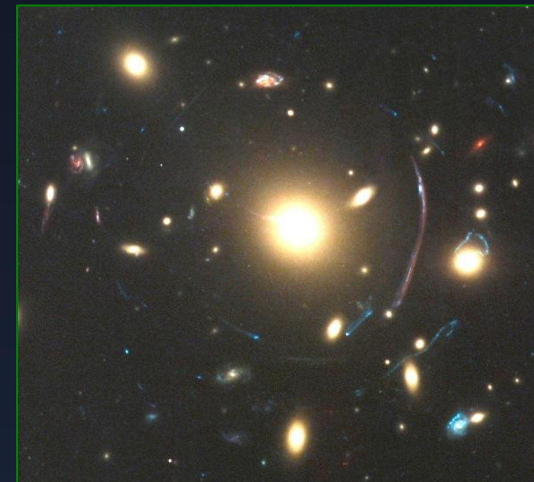

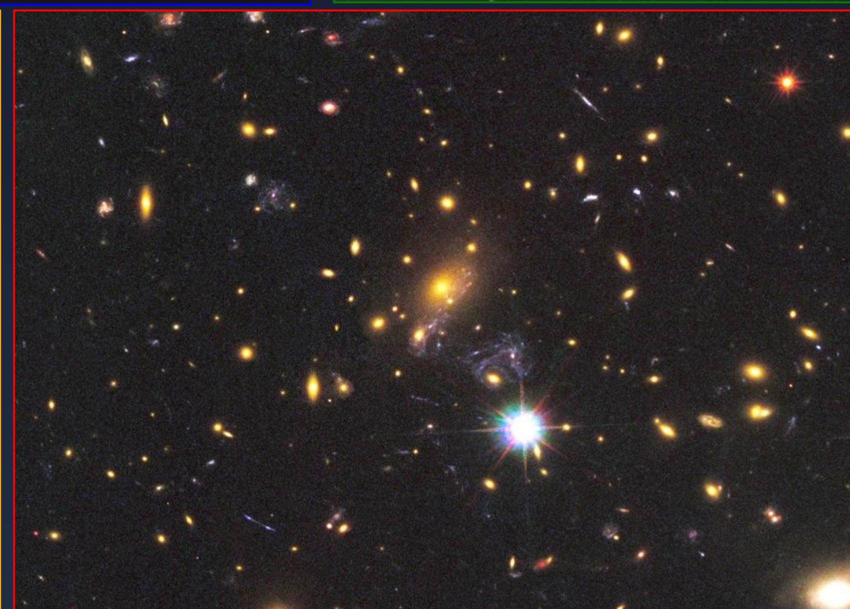

PI. Marc Postman (STScI)

http://www.stsci.edu/~postman/CLASH/Home.html

CLASH Objectives & Motivation

Before CLASH (2010), deep-multicolor Strong (*HST*) + Weak (*Subaru*) lensing data only available for a handful of "**super lens" clusters**

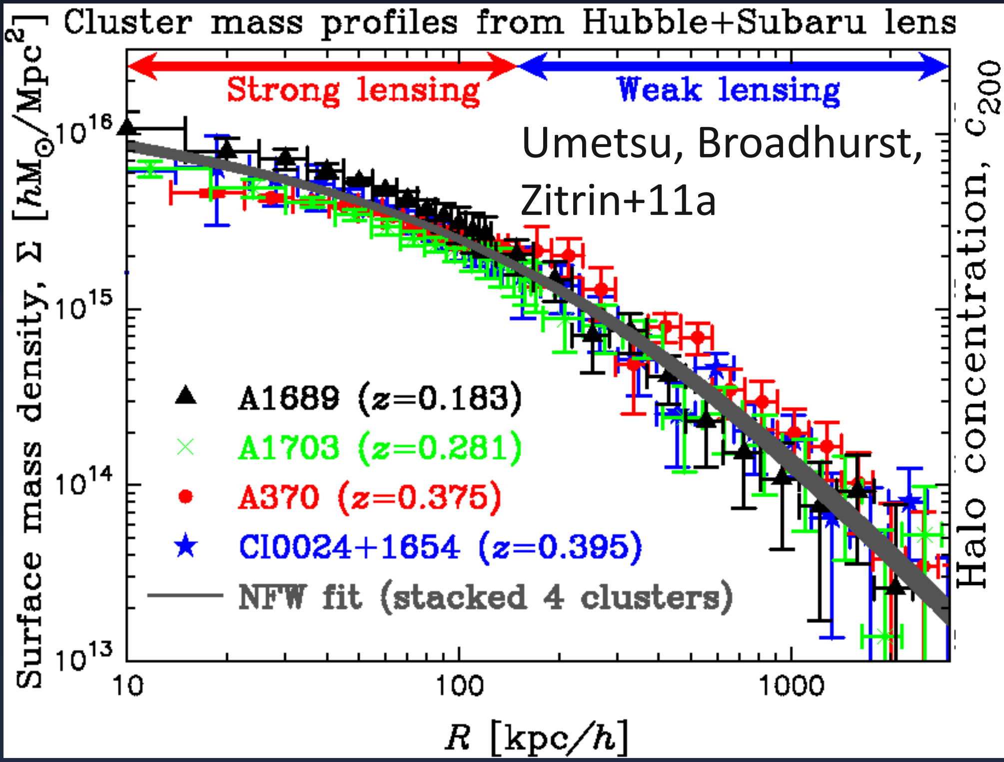

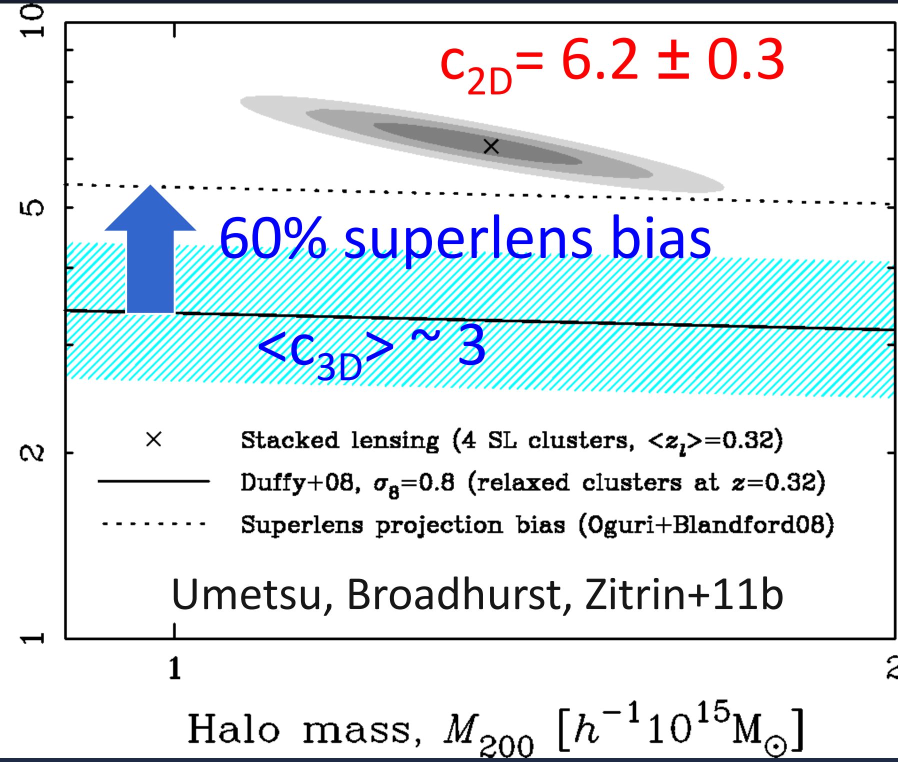

Total mass profile shape: consistent w self-similar NFW (cf. Newman+13; Okabe+13)
Degree of concentration: predicted superlens correction not enough if $<c_{LCDM}>$~3?

CLASH Objectives & Motivation

Before CLASH (2010), deep-multicolor Strong (*HST*) + Weak (*Subaru*) lensing data only available for a handful of “**superlens” clusters**

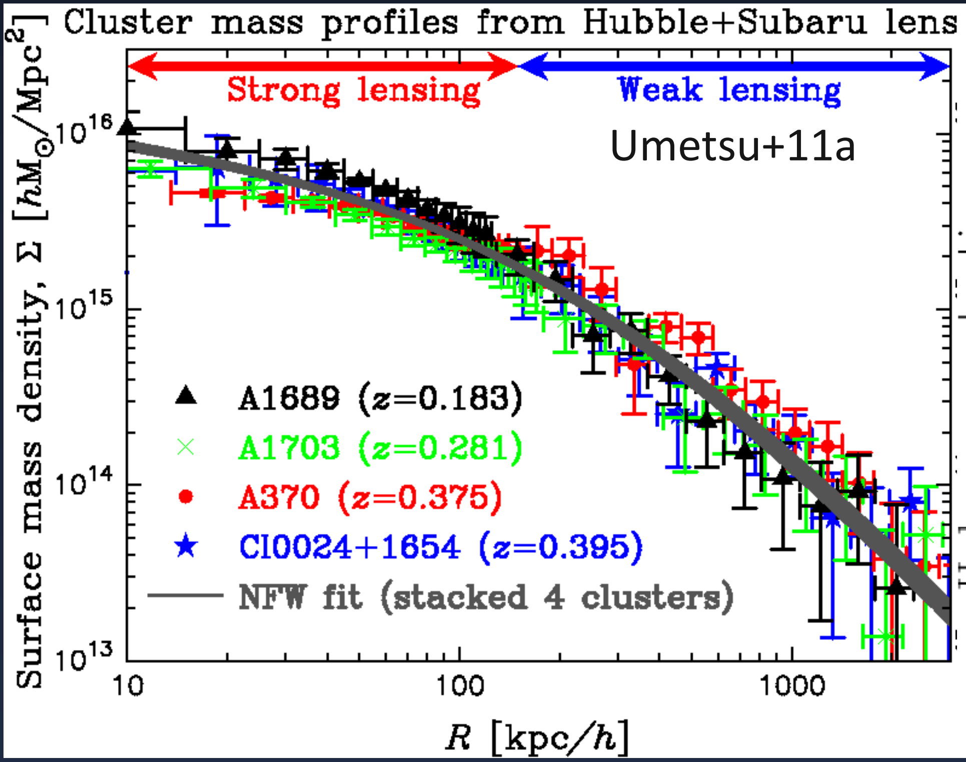

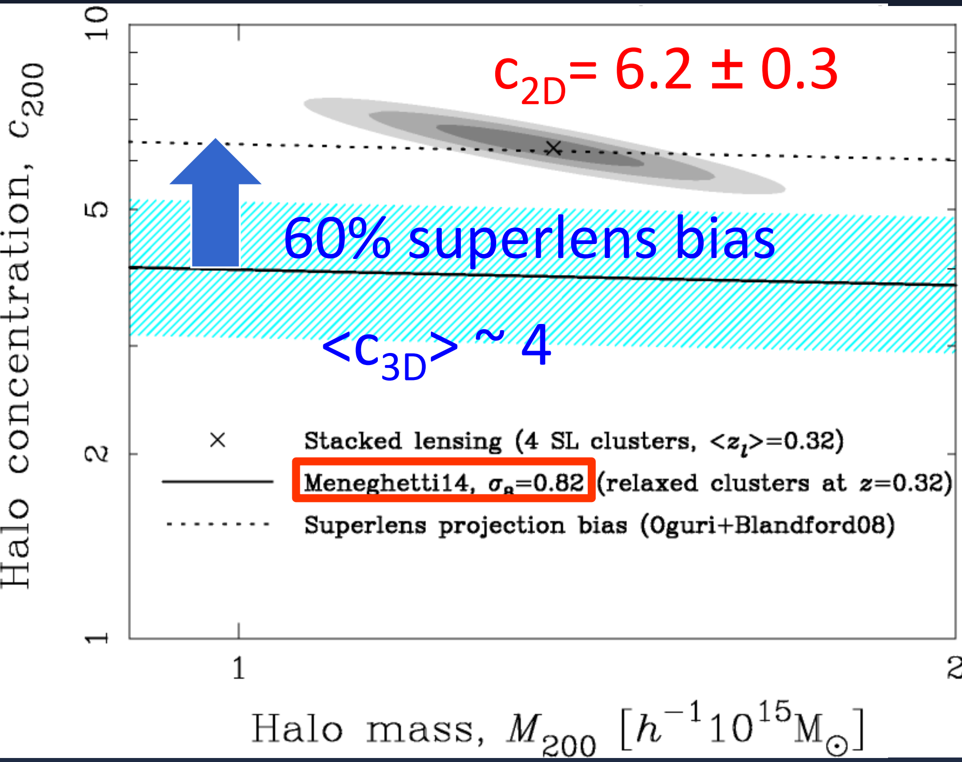

Total mass profile shape: consistent w self-similar NFW (cf. Newman+13; Okabe+13)
Degree of concentration: predicted superlens correction is just enough if $<c_{LCDM}>$~4

CLASH X-ray-selected Subsample

- **High-mass clusters with smooth X-ray morphology**
  - $T_x > 5$keV ($M_{200c} > 5e14 M_{sun}/h$)
  - Small BCG/X-ray peak offset, $\sigma_{off} \sim 10$kpc/h
  - Smooth regular X-ray morphology

  → Optimized for radial-profile analysis

- **CLASH theoretical predictions** (Meneghetti+14)
  - Composite relaxed (70%) and unrelaxed (30%) clusters
  - Mean $<c_{200c}>=3.9$, $c_{200c}=[3, 6]$
  - Small scatter in c_{200c} : $\sigma(\ln c_{200c}) = 0.16$
  - Largely free of orientation bias (~2% in $<M_{3D}>$)
  - >90% of CLASH clusters to have strong-lensing features

CLASH: Joint Analysis of Strong-lensing, Weak-lensing Shear and Magnification Data for 20 CLASH Galaxy Clusters

Umetsu et al. 2016, arXiv:1507.04385

Subaru/Suprime-Cam multi-color imaging for wide-field

High-resolution space imaging with *HST* (ACS/WFC3) for strong lensing

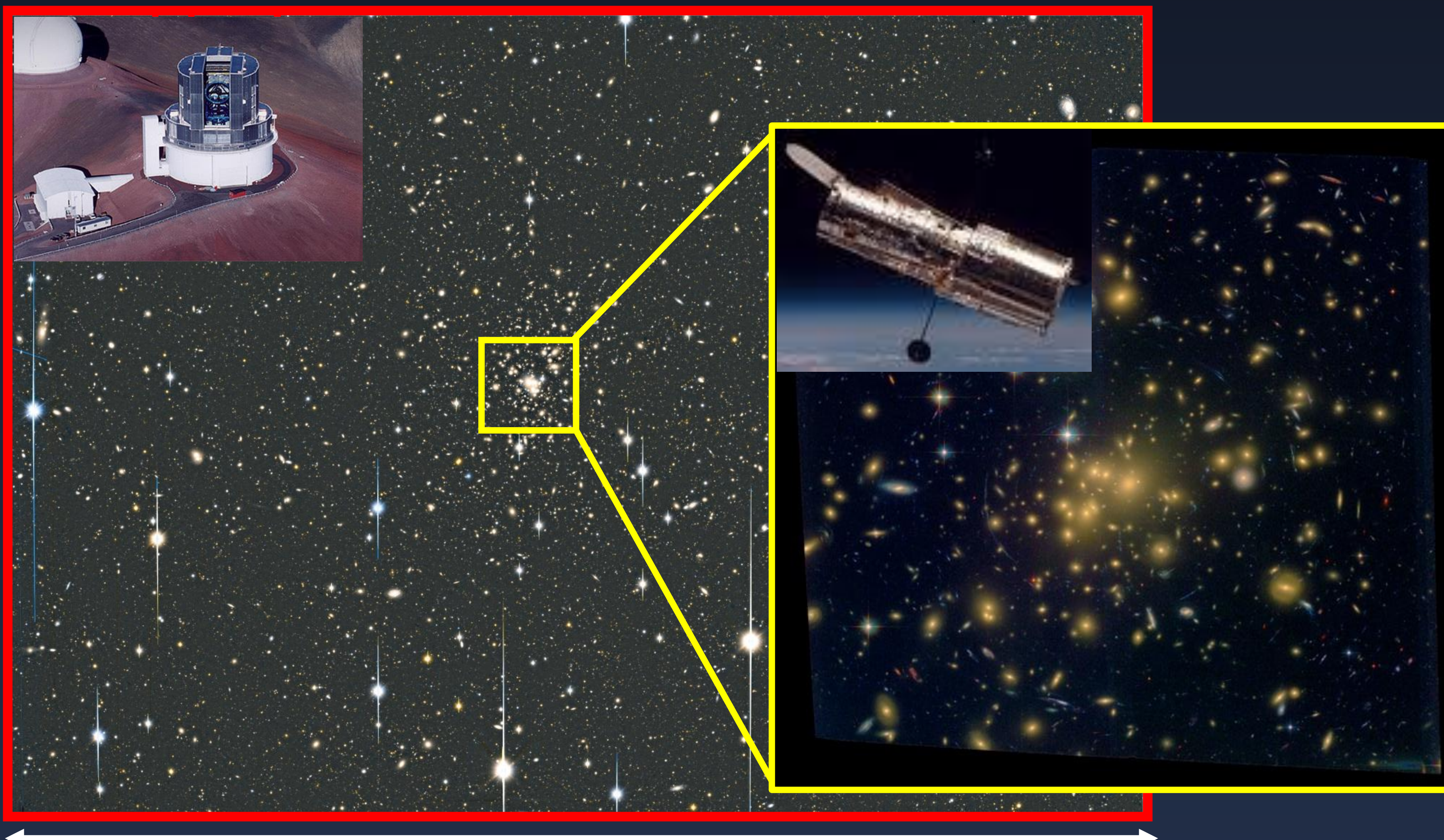

CLASH *Subaru* Weak-lensing Dataset

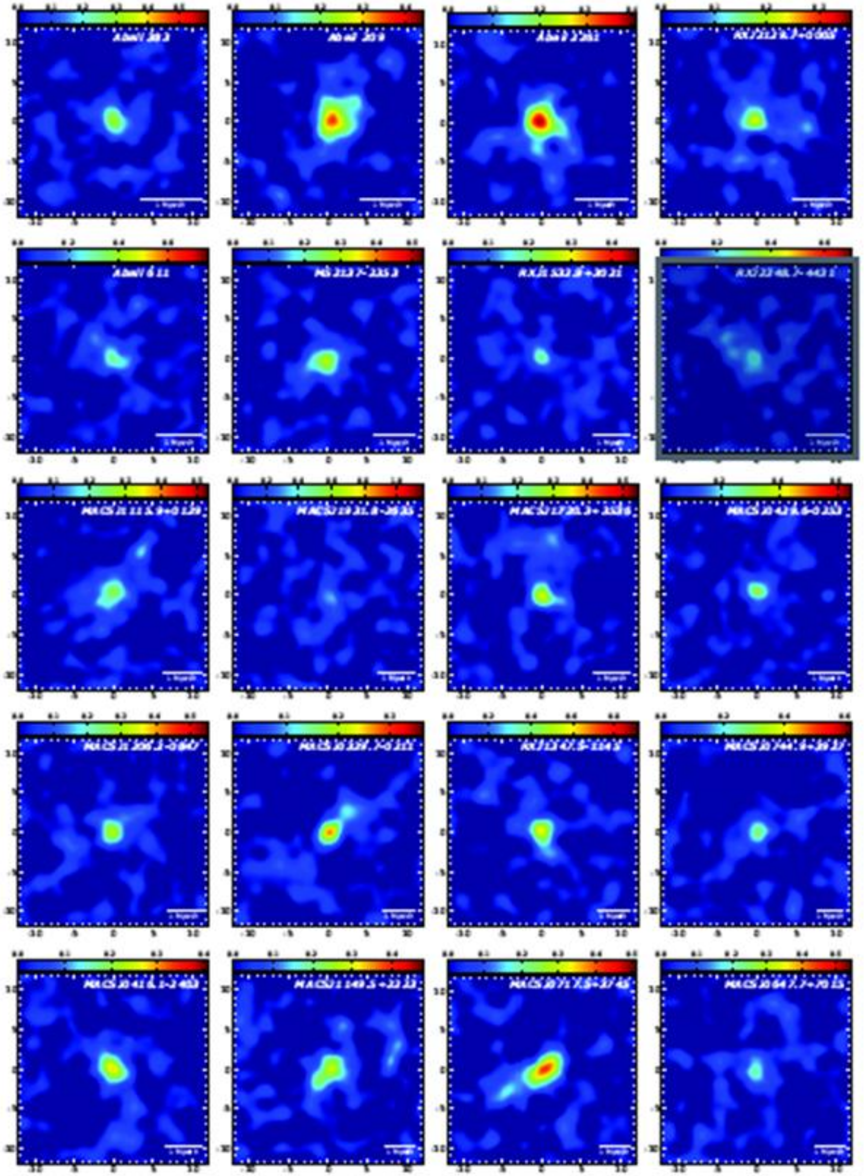

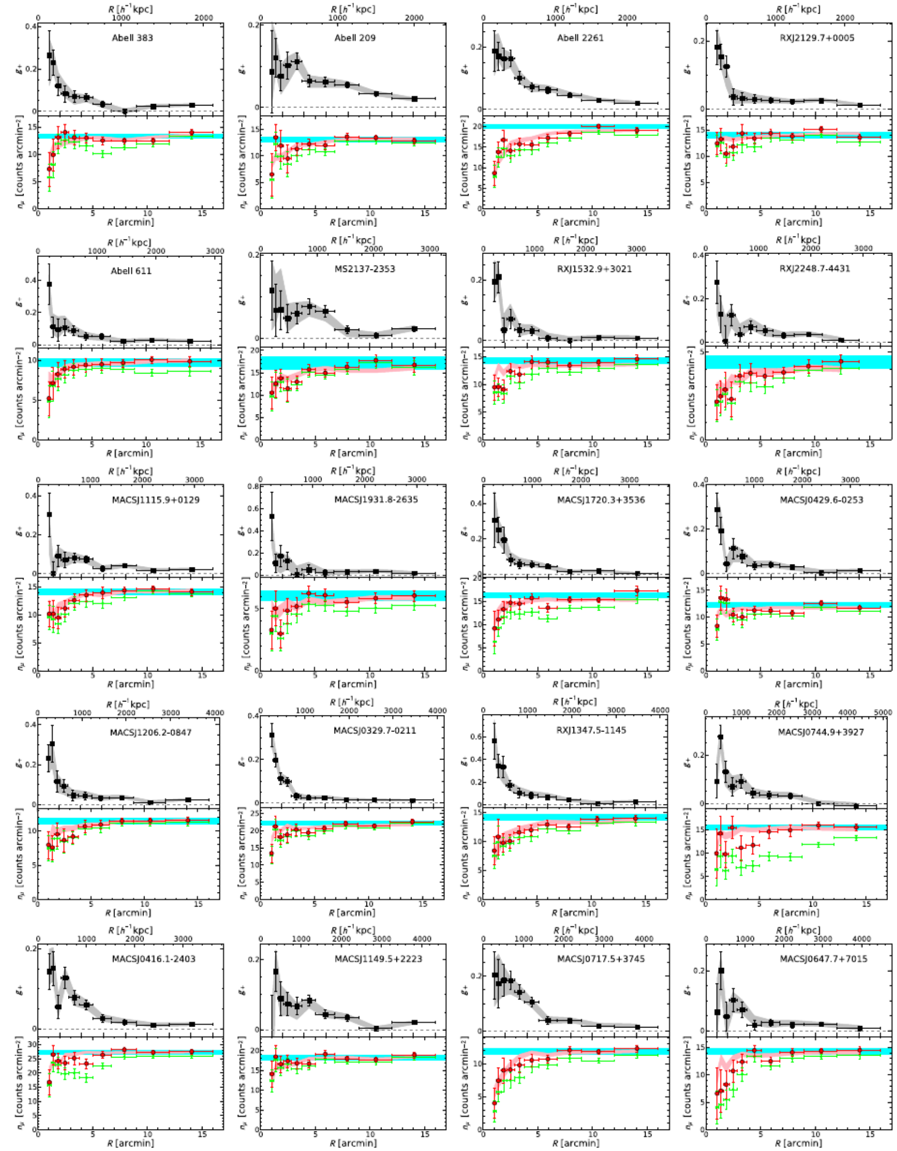

Umetsu, Medezinski, Nonino et al. 2014, *ApJ*, 795, 163

Joint Analysis of SL & WL shear+magnification

$$\{M_{2\mathrm{D},i}\}_{i=1}^{N_{\mathrm{SL}}}, \{\langle g_{+,i}\rangle\}_{i=1}^{N_{\mathrm{WL}}}, \{\langle n_{\mu,i}\rangle\}_{i=1}^{N_{\mathrm{WL}}}.$$

Determination of $M_{2D}(<R)$ from detailed *HST* SL modeling (Zitrin+15)

- Effective resolution: ΔR = 10"($<R_{\mathrm{Ein}}>$/22")($<N>$/17)$^{-1/2}$
- Maximum integration radius: R_{max} ~ 2$<R_{\mathrm{Ein}}>$ ~ 40"

HST-SL mass integration radii: *R*=(10", 20", 30", 40")

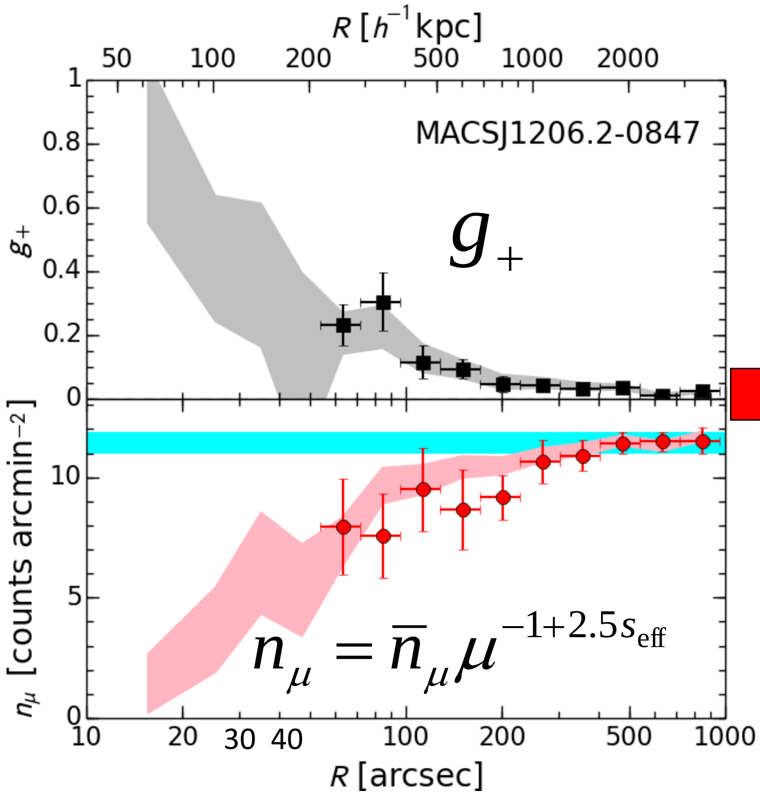

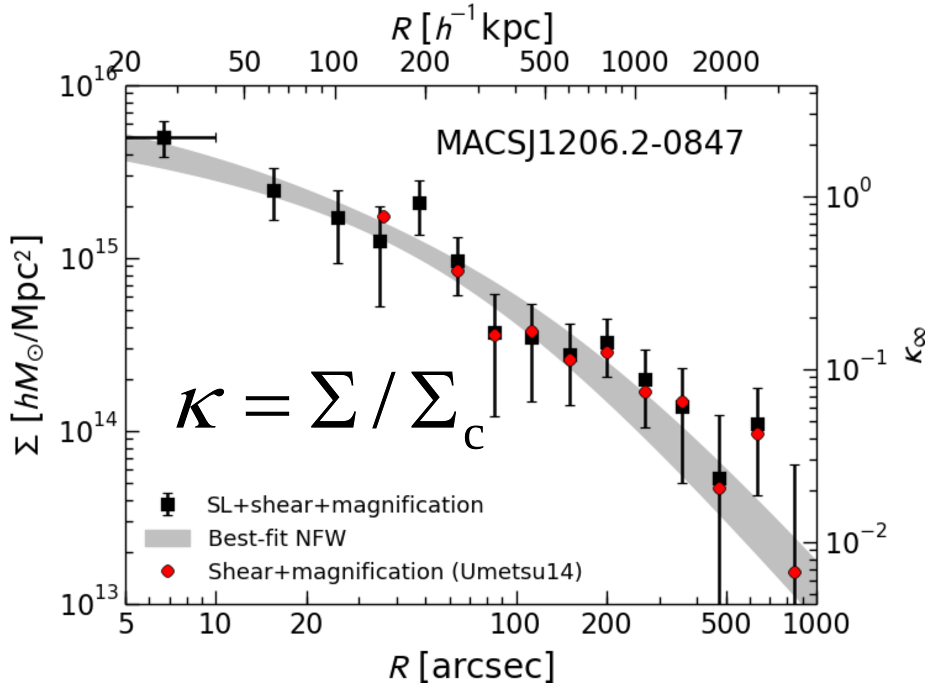

$<\chi^2$/dof$>$ = 0.95 for 20 CLASH clusters

CLASH Ensemble Mass Profile

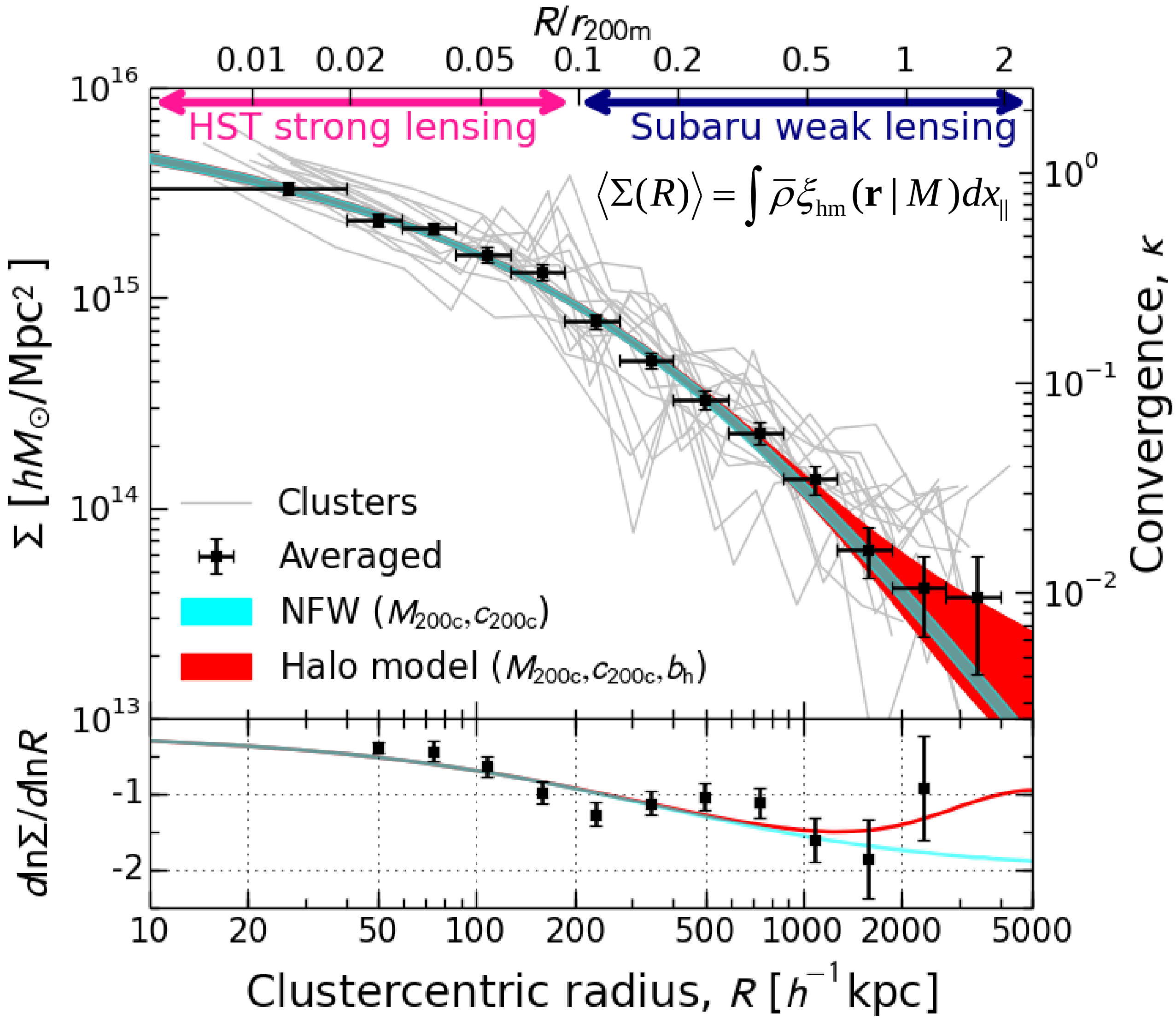

33σ detection of the ensemble-averaged mass profile out to ~2r_{200m}

Characterizing the Ensemble Mass Profile

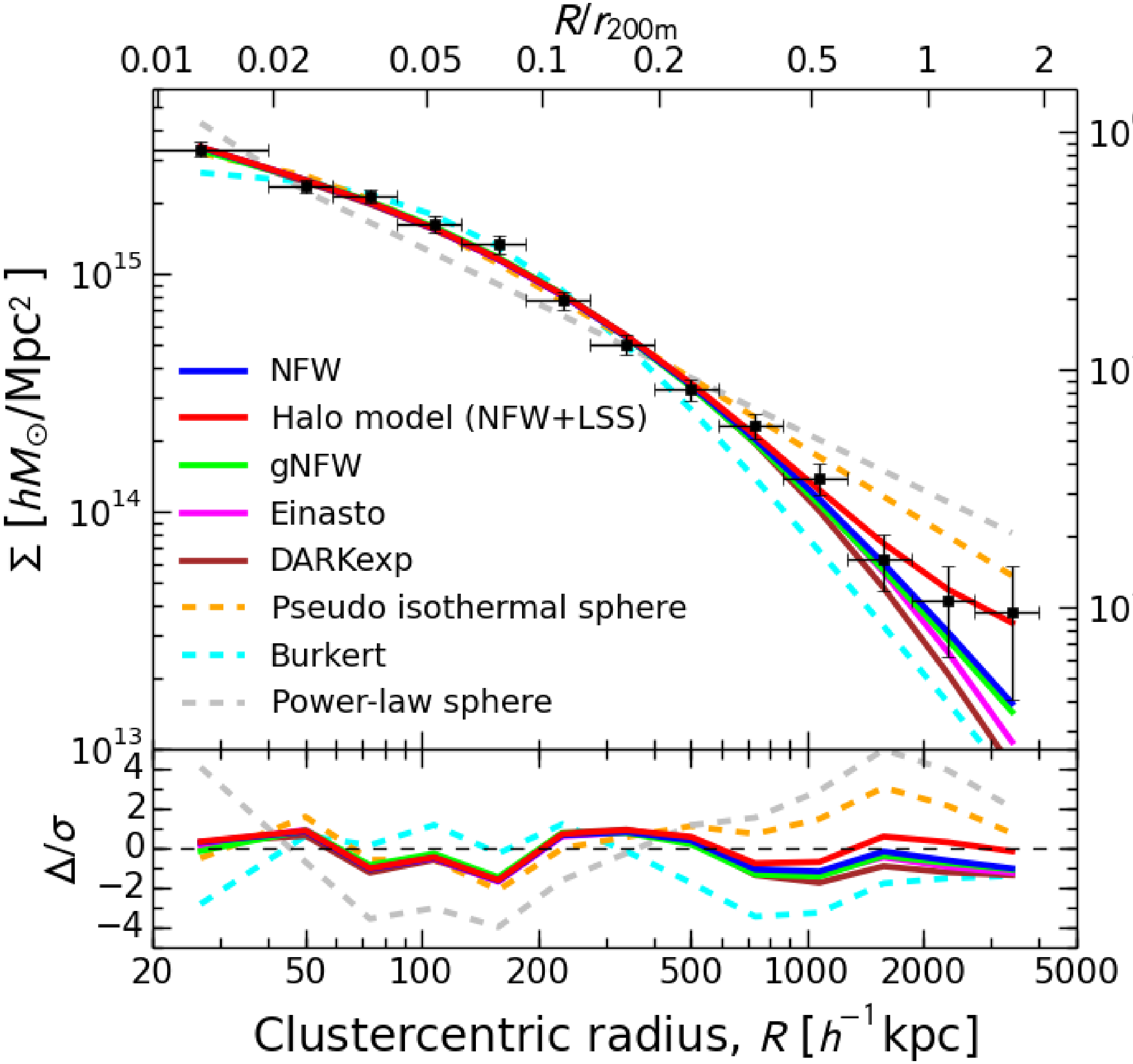

$$\Sigma(R) = \int dl\, \Delta\rho(r),$$

Models:

1. **No 2-halo term**
   (f_t=1, ρ_{2h}=0)
2. **With 2-halo term**
   (Tinker+10)

$$\Delta\rho(r) = f_t(r)\, \rho_h(r) + \rho_{2h}(r),$$

$$f_t(r) = \left[1 + \left(\frac{r}{r_t}\right)^2\right]^{-2},$$

Comparison of Best-fit Models

Acceptable fits: *p* values (PTE) > 0.05

Table 4
Best-fit models for the stacked mass profile of the CLASH X-ray-selected subsample

Model	M_{200c} ($10^{14} M_\odot\ h_{70}^{-1}$)	c_{200c}	Shape/structural parameters	b_h	χ^2/dof	PTE[a]	Notes
NFW	$14.4^{+1.1}_{-1.0}$	$3.76^{+0.29}_{-0.27}$	$\gamma_c = 1$	—	11.3/11	0.419	No truncation
gNFW	$14.1^{+1.1}_{-1.1}$	$4.04^{+0.53}_{-0.52}$	$\gamma_c = 0.85^{+0.22}_{-0.31}$	—	10.9/10	0.366	No truncation
Einasto	$14.7^{+1.1}_{-1.1}$	$3.53^{+0.36}_{-0.39}$	$\alpha_E = 0.232^{+0.042}_{-0.038}$	—	11.7/10	0.306	No truncation
DARKexp–γ[b]	$14.5^{+1.2}_{-1.1}$	$3.53^{+0.42}_{-0.42}$	$\phi_0 = 3.90^{+0.41}_{-0.45}$	—	13.5/10	0.198	No truncation
Pseudo isothermal	—	—	$V_c = 1762^{+40}_{-39}$ km/s, $r_c = 69^{+7}_{-7}$ kpc	—	23.6/11	0.015	No truncation
Burkert	$11.6^{+0.8}_{-0.8}$	—	$r_{200c}/r_0 = 8.81^{+0.42}_{-0.41}$	—	29.9/11	0.002	No truncation
Power-law sphere	$12.5^{+0.8}_{-0.8}$	—	$\gamma_c = 1.78^{+0.02}_{-0.02}$	—	93.5/11	0.000	No truncation
Halo model[c]:							
NFW+LSS (i)	$14.1^{+1.0}_{-1.0}$	$3.79^{+0.30}_{-0.28}$	$\gamma_c = 1$	9.3	10.9/11	0.450	ΛCDM $b_h(M)$ scaling
NFW+LSS (ii)	$14.4^{+1.4}_{-1.3}$	$3.74^{+0.33}_{-0.30}$	$\gamma_c = 1$	$7.4^{+4.6}_{-4.7}$	10.8/10	0.377	b_h as a free parameter
Einasto+LSS (i)	$14.3^{+1.1}_{-1.1}$	$3.69^{+0.36}_{-0.42}$	$\alpha_E = 0.248^{+0.051}_{-0.047}$	9.3	10.7/10	0.385	ΛCDM $b_h(M)$ scaling
Einasto+LSS (ii)	$14.5^{+1.9}_{-1.6}$	$3.65^{+0.47}_{-0.61}$	$\alpha_E = 0.245^{+0.061}_{-0.053}$	$8.7^{+5.3}_{-5.6}$	10.6/9	0.301	b_h as a free parameter
DARKexp+LSS (i)	$14.2^{+1.2}_{-1.1}$	$3.64^{+0.44}_{-0.46}$	$\phi_0 = 3.89^{+0.51}_{-0.54}$	9.3	11.7/10	0.308	ΛCDM $b_h(M)$ scaling
DARKexp+LSS (ii)	$14.0^{+1.8}_{-1.6}$	$3.69^{+0.53}_{-0.57}$	$\phi_0 = 3.85^{+0.57}_{-0.61}$	$10.1^{+4.9}_{-5.1}$	11.6/9	0.235	b_h as a free parameter

[a] Probability to exceed the observed χ^2 value.
[b] We use Dehnen–Tremaine γ-models with the central cusp slope $\gamma_c = 3\log_{10}\phi_0 - 0.65$ ($1.7 \le \phi_0 \le 6$) as an analytic fitting function for the DARKexp density profile.
[c] For halo model predictions, we decompose the total mass overdensity $\Delta\rho(r) = \rho(r) - \overline{\rho}_m$ as $\Delta\rho = f_t\rho_h + \rho_{2h}$ where $\rho_h(r)$ is the halo density profile, $\rho_{2h}(r) = \overline{\rho}_m b_h \xi_m^L(r)$ is the two-halo term, and $f_t(r) = (1 + r^2/r_t^2)^{-2}$ describes the steepening of the density profile in the transition regime around the truncation radius r_t, which is assumed to be $r_t = 3r_{200c}$.

- Consistent with cuspy density profiles (NFW, Einasto, DARKexp)
- Cuspy models that include ΛCDM 2-halo term (b_h~9.3) give improved fits

CLASH *Concentration vs. Mass* Relation

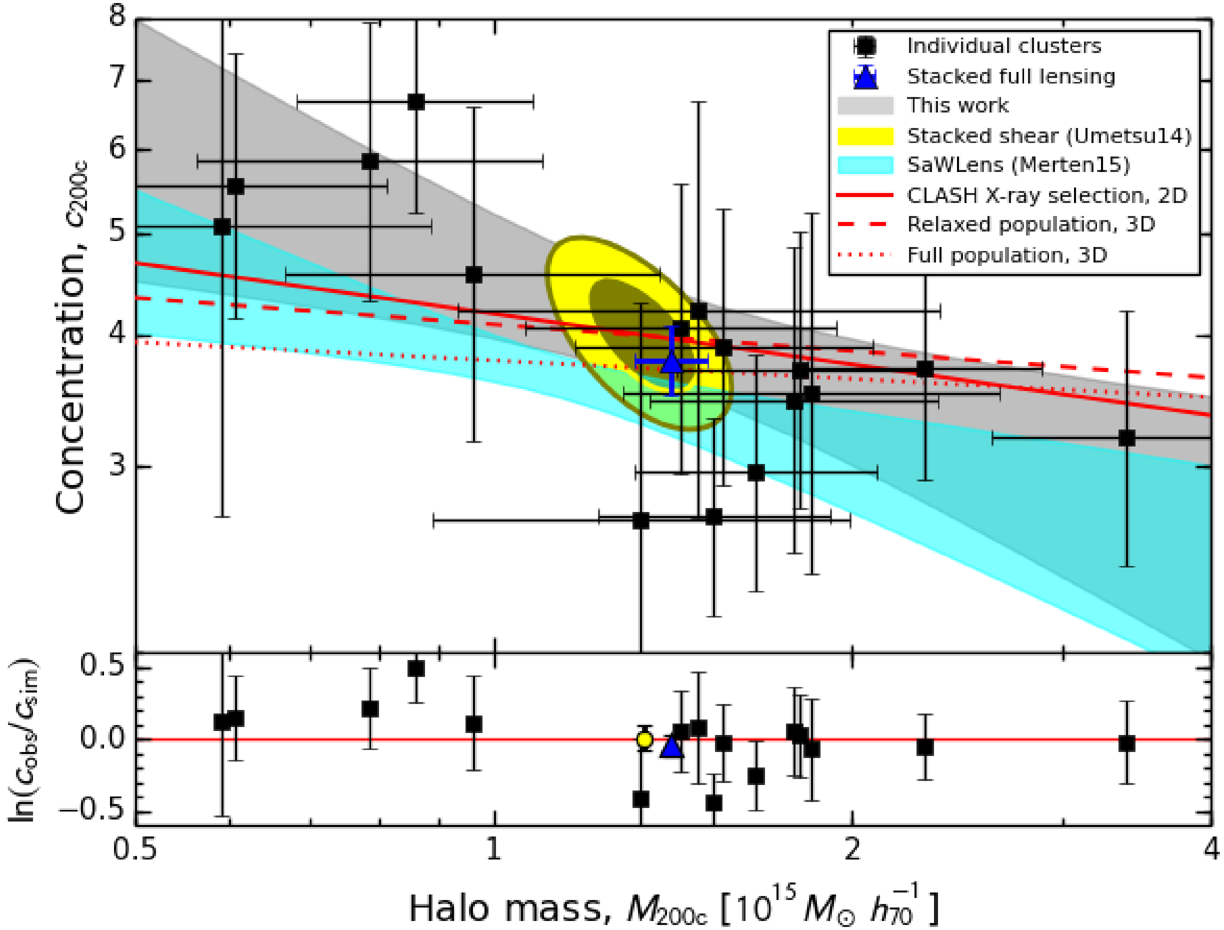

Predicted (M14):

$$\langle c_{200c} \rangle = 3.9,$$

$$3 \le c_{200c} \le 6,$$

$$\sigma(\ln c_{200_c}) = 0.16$$

Observed:

$$c_{200c}|_{z=0.34} = 3.95 \pm 0.35$$

$$\text{at } M_{200c} = 10^{15} M_{sun}/h,$$

$$\sigma(\ln c_{200_c}) = 0.13 \pm 0.06$$

Normalization, slope, & scatter are all consistent with LCDM when the CLASH selection function based on X-ray morphological regularity and the projection effects are taken into account

Comparison with LCDM $c(M)$ models

Table 5
Comparison of measured and predicted concentrations for the CLASH X-ray-selected subsample

Author	Sample	3D/2D	Function[a]	$c^{(\mathrm{obs})}/c^{(\mathrm{pred})}$ Average[c]	σ[d]	χ^2	PTE[b]
Theory:							
Duffy et al. (2008)	full	3D	c–M	1.331 ± 0.108	0.334	22.6	0.046
Duffy et al. (2008)	relaxed	3D	c–M	1.165 ± 0.094	0.290	13.6	0.399
Prada et al. (2012)	full	3D	c–ν	0.733 ± 0.065	0.244	24.6	0.026
Bhattacharya et al. (2013)	full	3D	c–ν	1.169 ± 0.095	0.292	14.1	0.369
Bhattacharya et al. (2013)	relaxed	3D	c–ν	1.131 ± 0.092	0.277	12.4	0.494
Dutton & Macciò (2014)	full	3D	c–M	1.061 ± 0.086	0.262	10.4	0.659
Meneghetti et al. (2014)	full	3D	c–M	1.061 ± 0.089	0.279	10.2	0.675
Meneghetti et al. (2014)	relaxed	3D	c–M	0.990 ± 0.083	0.249	9.2	0.760
Diemer & Kravtsov (2015)	full (median)	3D	c–ν	1.021 ± 0.083	0.330	14.4	0.349
Diemer & Kravtsov (2015)	full (mean)	3D	c–ν	1.060 ± 0.086	0.326	13.8	0.391
Meneghetti et al. (2014)	full	2D	c–M	1.087 ± 0.092	0.336	13.5	0.413
Meneghetti et al. (2014)	relaxed	2D	c–M	1.040 ± 0.086	0.283	10.8	0.628
Meneghetti et al. (2014)	CLASH	2D	c–M	0.988 ± 0.078	0.227	9.6	0.730
Observations:							
Merten et al. (2015)	CLASH	2D	c–M	1.133 ± 0.087	0.209	9.2	0.754

WMAP5

[a] c–M: power-law $c(M, z)$ relation; c–ν: halo concentration given as a function of peak height $\nu(M, z)$.
[b] Probability to exceed the measured χ^2 value assuming the standard χ^2 probability distribution function.
[c] Weighted geometric average of observed-to-predicted concentration ratios.
[d] Standard deviation of the distribution of observed-to-predicted concentration ratios.

High normalization

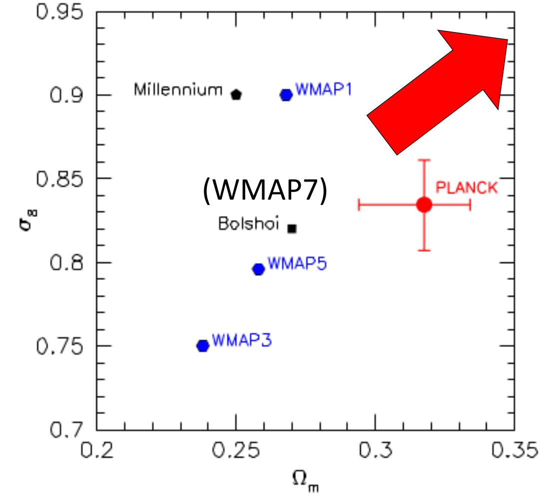

- Consistent with models that are calibrated for more recent cosmologies (WMAP7 and later)
- Better agreement is achieved when selection effects (overall degree of relaxation) are taken into account

X-ray regular vs. Superlens Clusters

Umetsu+11b: 4 *superlens*es with $R_{\rm Ein}$>30” at z_s=2 (A1689, A1703, Cl0024, A370)

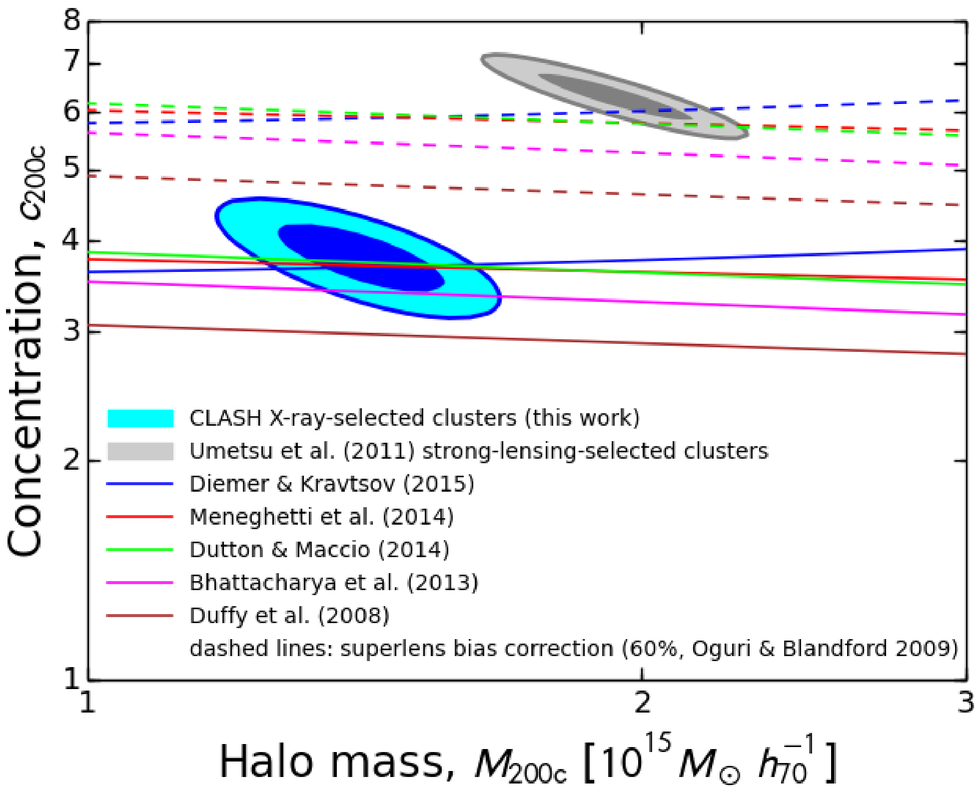

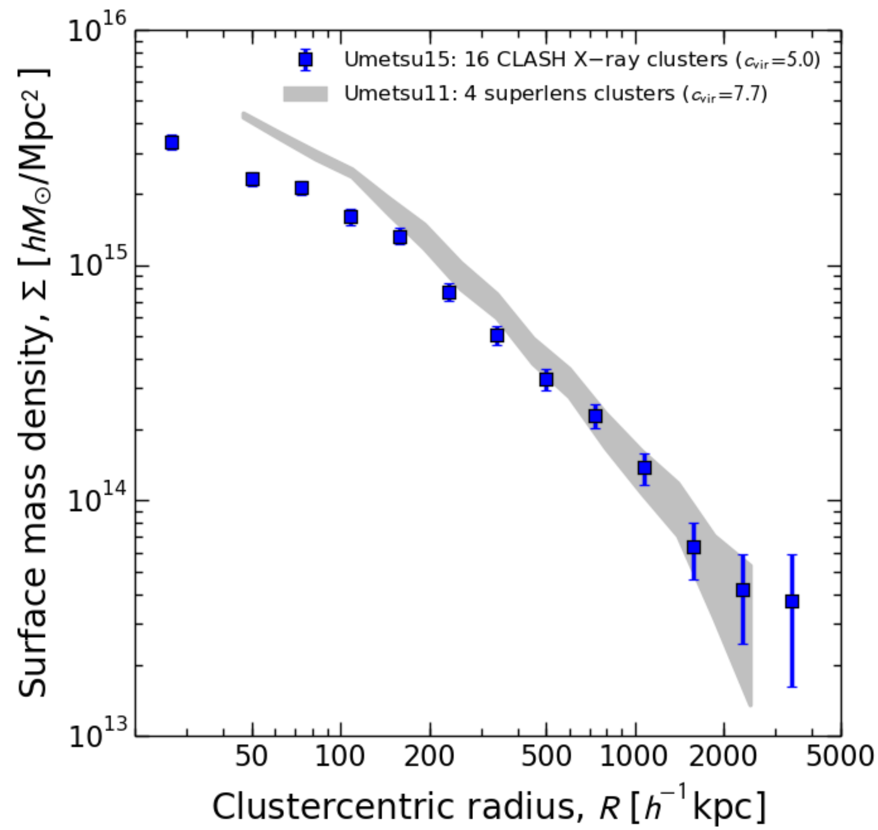

Higher normalization LCDM cosmology (WMAP7 and later) + “predicted” +60% superlens correction (e.g., Oguri+Blandford09) can explain superlens mass profiles!

Ensemble Calibration of Cluster Masses

Planck13 CMB vs. Cluster Cosmology

b=0.2?? – 0.4??

- Planck: 3σ tension between SZ cluster counts and CMB cosmology
- assumes M_{Planck} / M_{true} = (1-b) = 0.8
- calibrated with XMM hydrostatic masses (Arnaud et al. 2010) + simulations

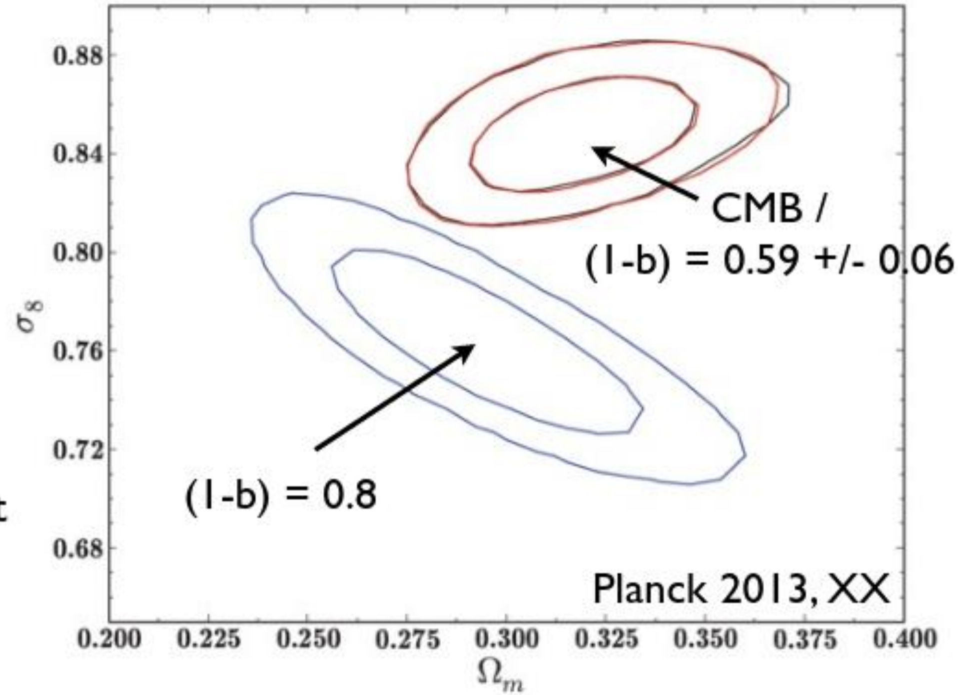

suggested explanations:

- mass bias underestimated (and no accounting for uncertainties)
- 2.9σ detection of neutrino masses: Σm_ν = (0.58 +/- 0.20) eV (Planck+WMAPpol+ACT+BAO: Σm_ν < 0.23 eV, 95% CL)

Slide taken from Anja von der Linden's presentation

Comparison with *Planck* Masses – Not so Simple

Mass-dependent bias (20-45%) observed for *Planck* mass estimates

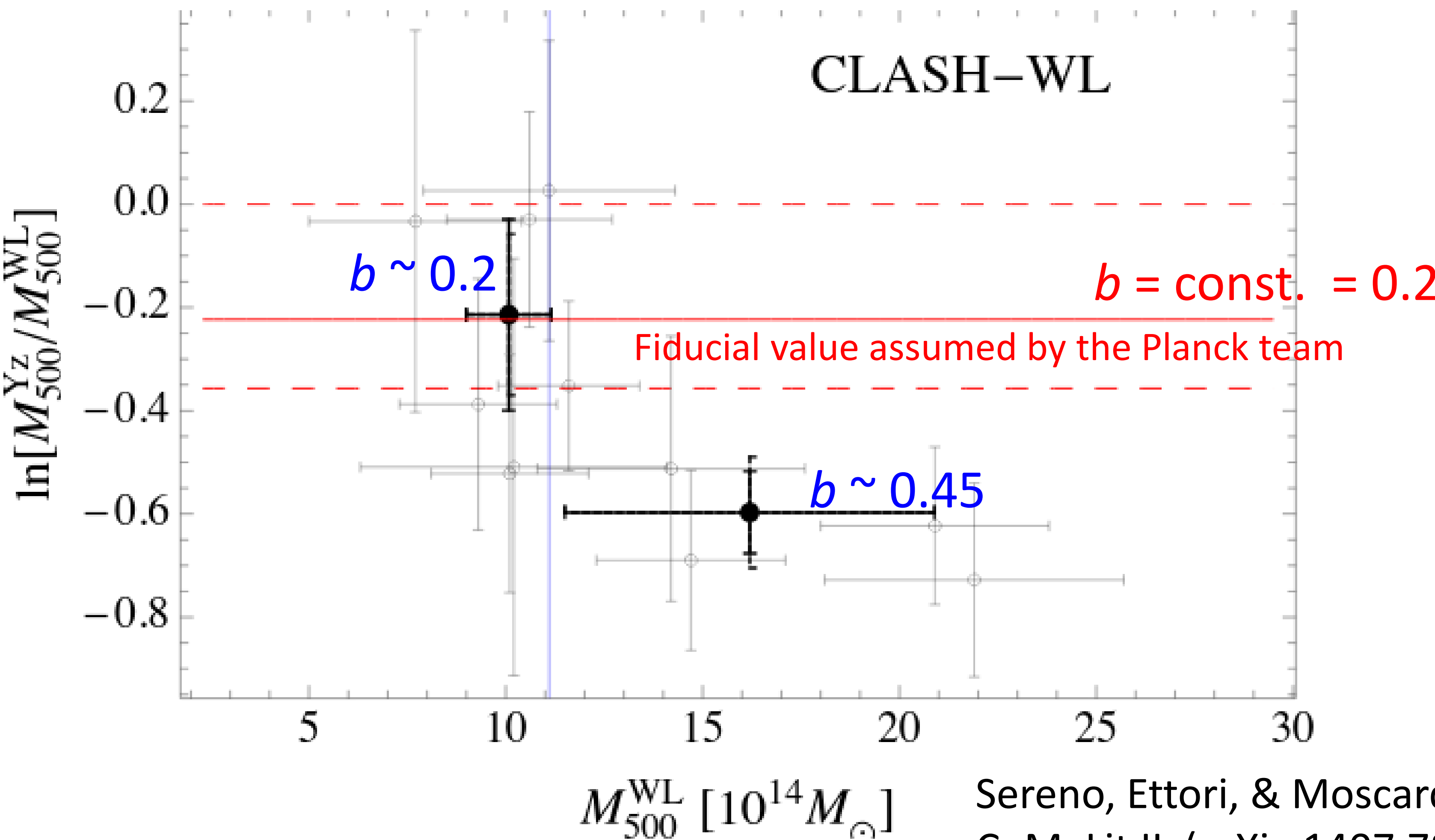

Sereno, Ettori, & Moscardini 15, CoMaLit II (arXiv:1407.7869)

CLASH Internal Consistency

$M_{3D}(<r)$ de-projected assuming spherical NFW density profiles

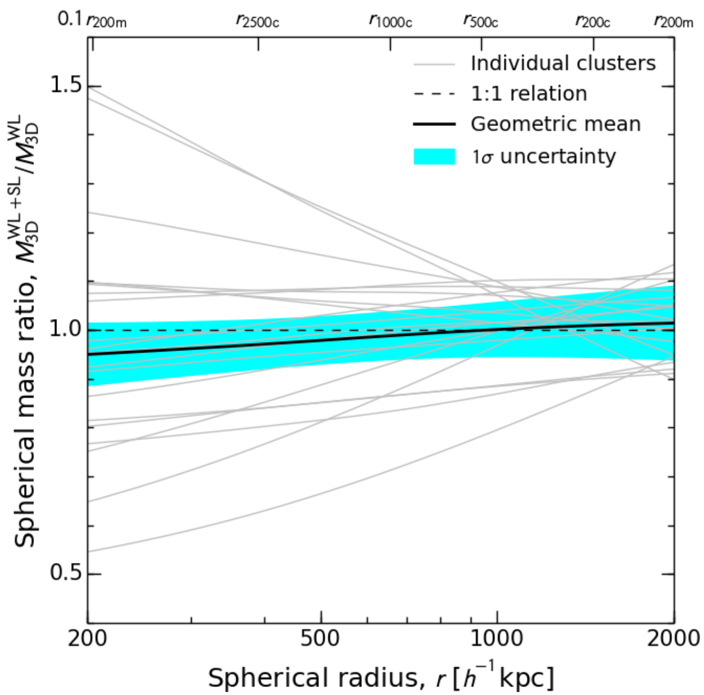

WL (U14) and WL+SL (U16) are consistent within 5% at *r* = [200, 2000] kpc/h

Umetsu+16, arXiv:1507.04385

CLASH ensemble mass calibration uncertainty

- Statistical uncertainty with *N*=20 clusters: 28%/sqrt(20) =6.3%
- Systematic uncertainty: 5.6% (5% shear calibration, 2% dilution)
- Mass modeling bias (deviations from NFW, orientation bias): 3%
- Total calibration uncertainty: 9%

Comparisons with Other WL Surveys

WtG [Subaru]
(Applegate+14)

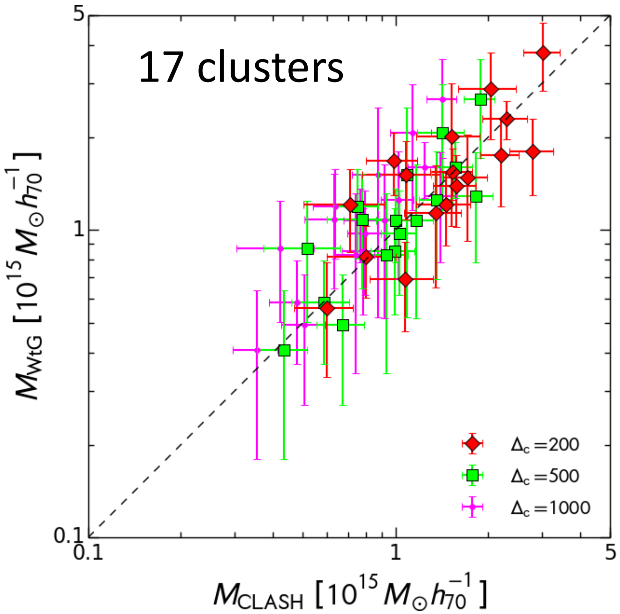

LoCuSS [Subaru]
(Okabe & Smith 15)

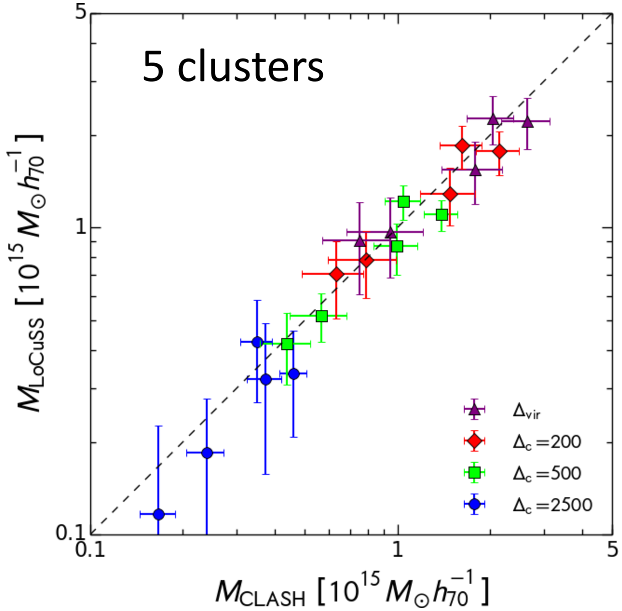

CCCP [CFHT]
(Hoekstra+15)

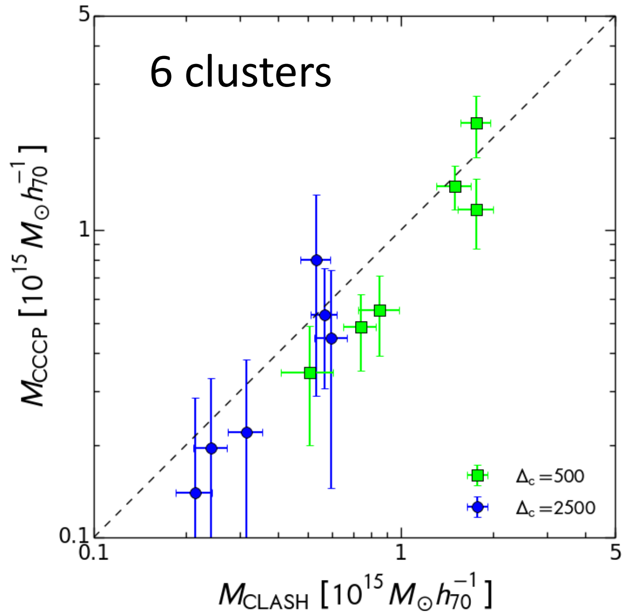

$$\langle M_{\rm WtG}/M_{\rm CLASH}\rangle = 1.03 \pm 0.09 \quad (\Delta = 200)$$
$$= 1.07 \pm 1.12 \quad (\Delta = 500)$$
$$= 1.07 \pm 1.12 \quad (\Delta = 1000)$$

$$\langle M_{\rm LoCuSS}/M_{\rm CLASH}\rangle = 1.00 \pm 0.15 \quad (\Delta = \Delta_{\rm vir})$$
$$= 0.98 \pm 0.13 \quad (\Delta = 200)$$
$$= 0.93 \pm 0.10 \quad (\Delta = 500)$$
$$= 0.84 \pm 0.22 \quad (\Delta = 2500)$$

$$\langle M_{\rm CCCP}/M_{\rm CLASH}\rangle = 0.84 \pm 0.10 \quad (\Delta = 500)$$
$$= 0.91 \pm 0.24 \quad (\Delta = 2500)$$

Umetsu+16,
arXiv:1507.04385

Summary

– Ensemble mass profile shape

- Data favor cuspy density profiles predicted for collisionless-DM-dominated halos in gravitational equilibrium (NFW, Einasto, DARKexp)
- The highest-ranked model is the 2-parameter NFW+LSS model including the 2-halo term using the LCDM *b*-*M* relation (b_{h} ~ 9.3)
- c_{200c} = 3.8 +/- 0.3 at $M_{200c}=10^{15} M_{\mathrm{sun}}/h$, z=0.34

– Concentration vs. mass relation

- Fully consistent with LCDM when the CLASH selection function based on X-ray morphological regularity and projection effects are taken into account

– Ensemble mass calibration

- Internal consistency (WL vs. WL+SL) at the ~5% level
- Total calibration uncertainty ~9% (~6% stat., ~6% sys.)

Supplemental Slides

Reionization Lensing Cluster Survey (RELICS)

Newly approved 190-orbit *HST* survey (7 ACS/WFC3 filters) of 41 high-mass clusters primarily selected from the *Planck* survey (P.I. Dan Coe; Oct 2015 – Apr 2017)

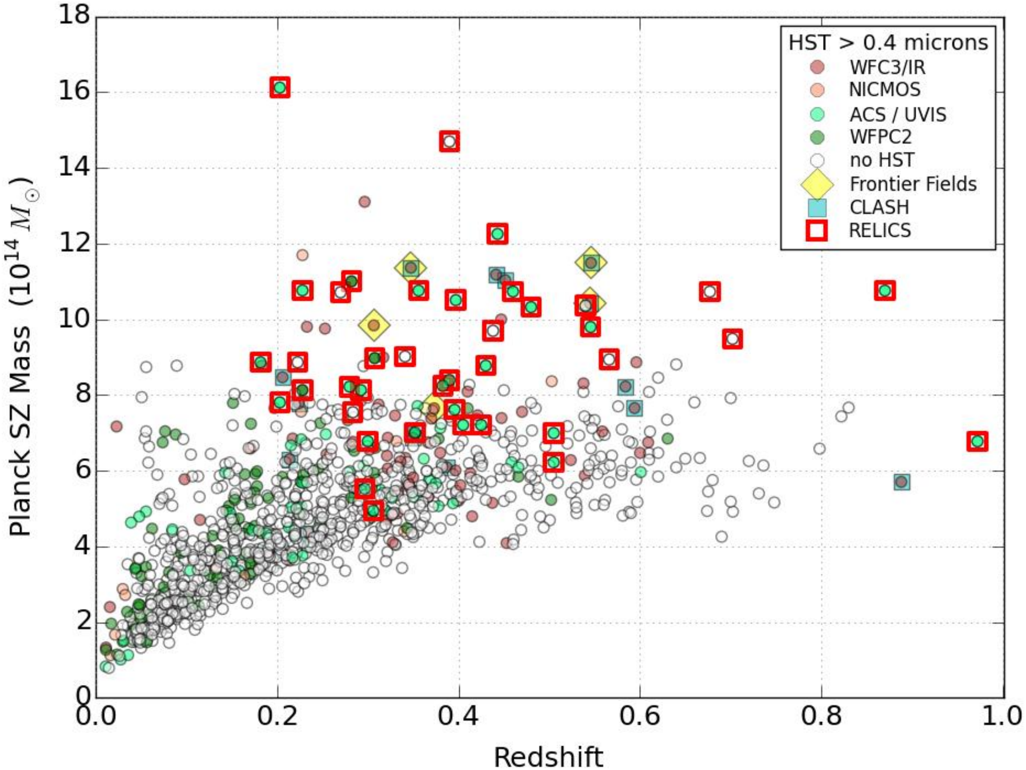

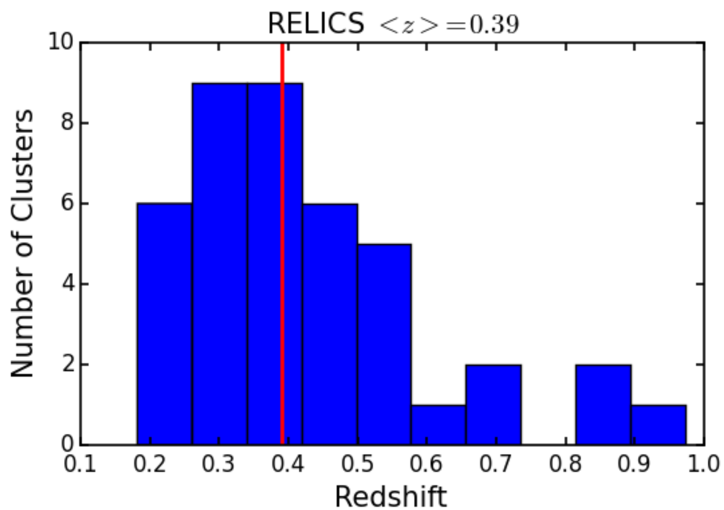

http://hstrelics.weebly.com

Ensemble-averaged Error Budget

Diagonal elements (C_{ii}) averaged over all CLASH clusters

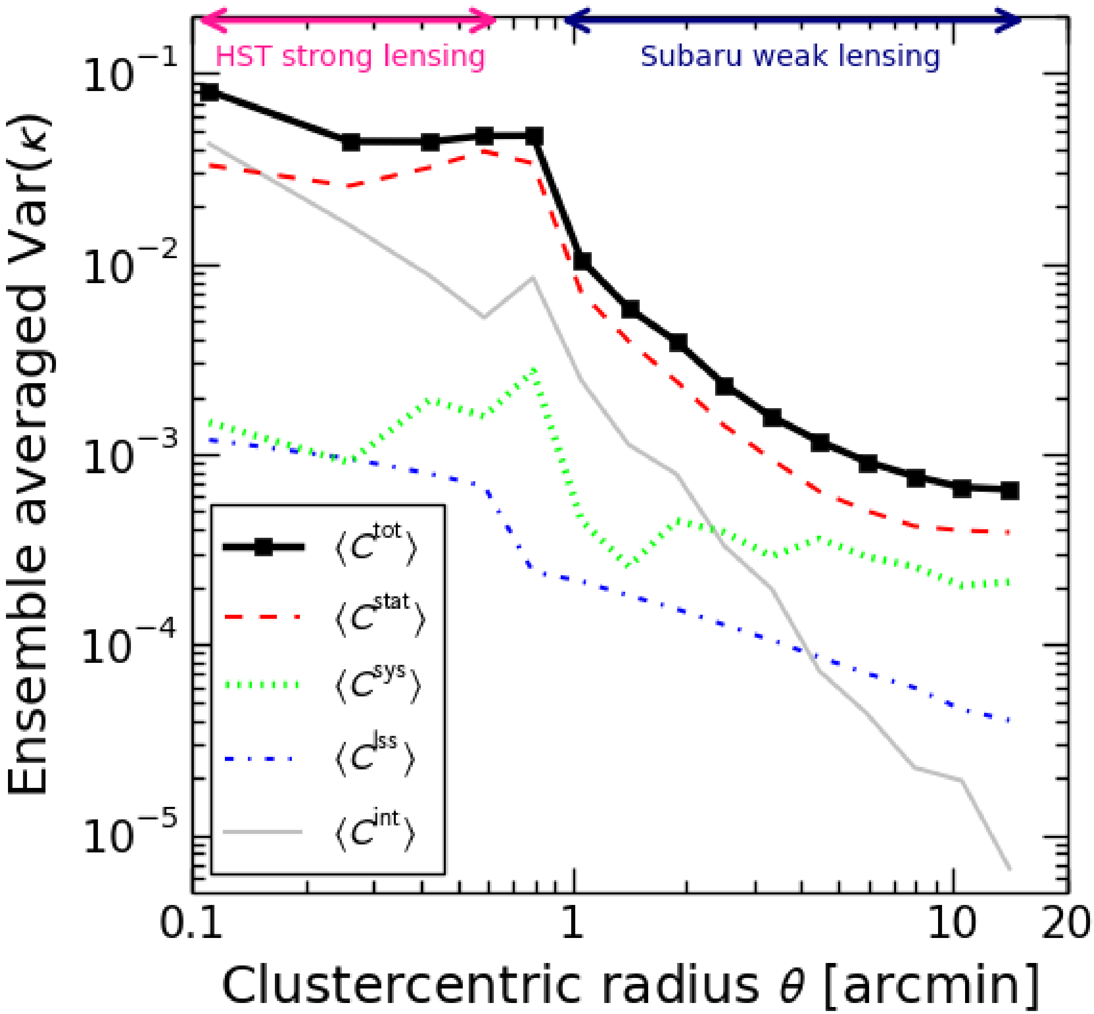

Residual mass-sheet uncertainty (Umetsu+14)

$$\left(C_{\rm sys}\right)_{ii} \sim \text{const.} \sim (0.02)^2$$

Intrinsic profile variations due to triaxiality, substructure, and *c*-*M* scatter (Gruen+15)

$$\left(C_{\rm int}\right)_{ii} \approx (0.2)^2 \kappa_i^2$$

Degree of Mass Concentration

$$c_{200} \equiv \frac{r_{200}}{r_s} = \frac{\text{(Outer scale radius)}}{\text{(Inner scale radius)}}$$

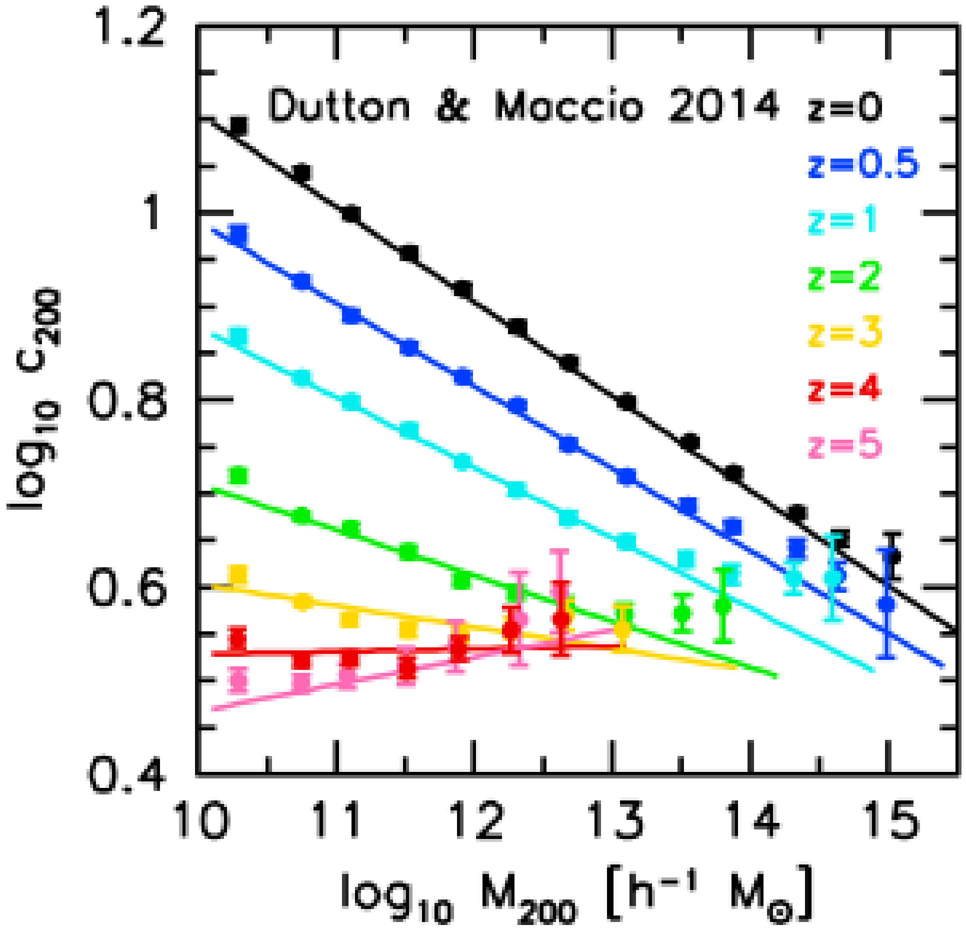

In hierarchical structure formation, <*c*> is predicted to correlate with *M*

- DM halos that are more massive collapse later on average, when the mean background density of the universe is correspondingly lower (e.g., Bullock+01)

Concentration is sensitive to cosmology

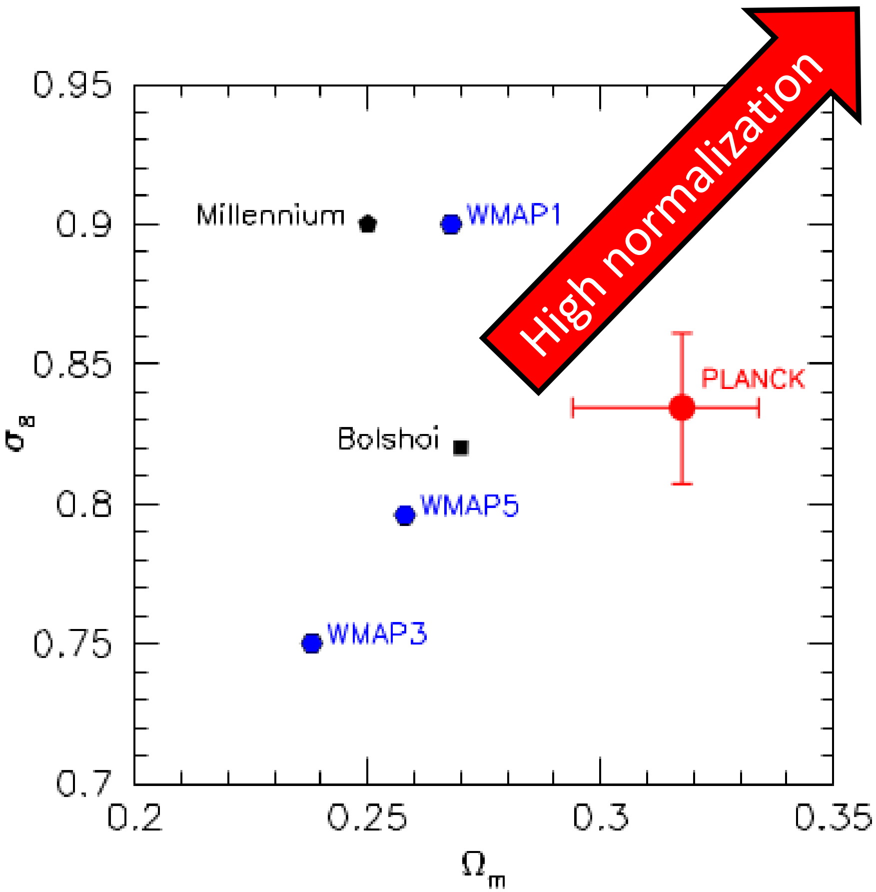

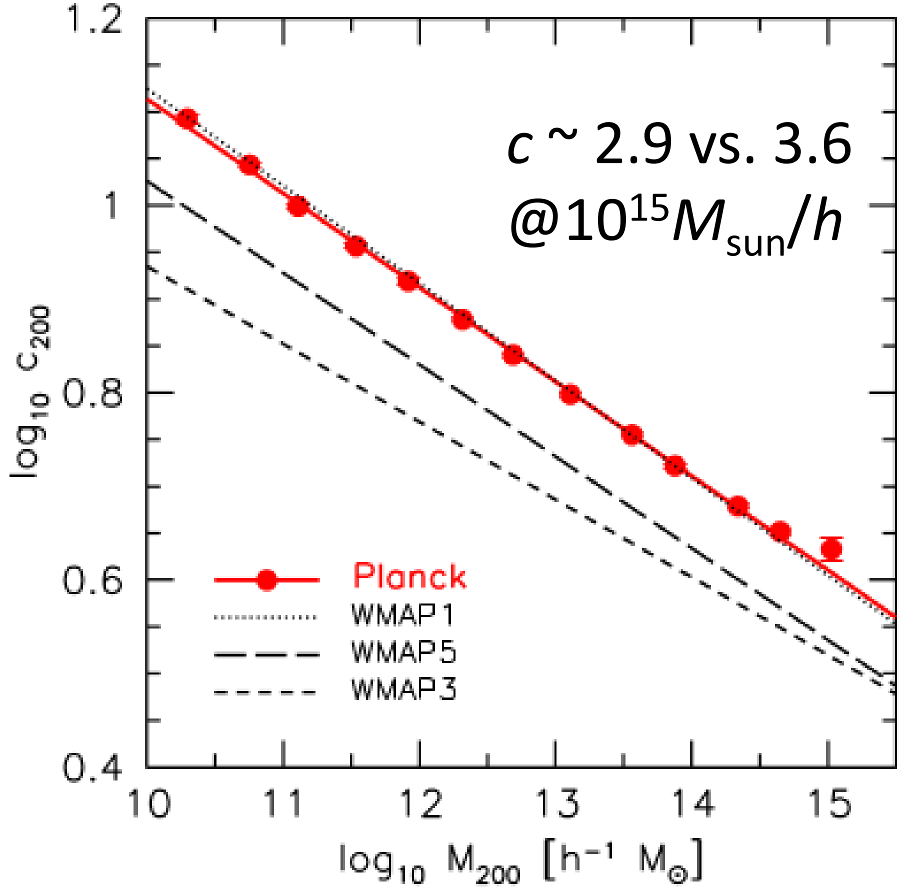

Dutton & Maccio 2014

Intrinsic Scatter in $c(M)$: Mass Assembly Histories (MAH)

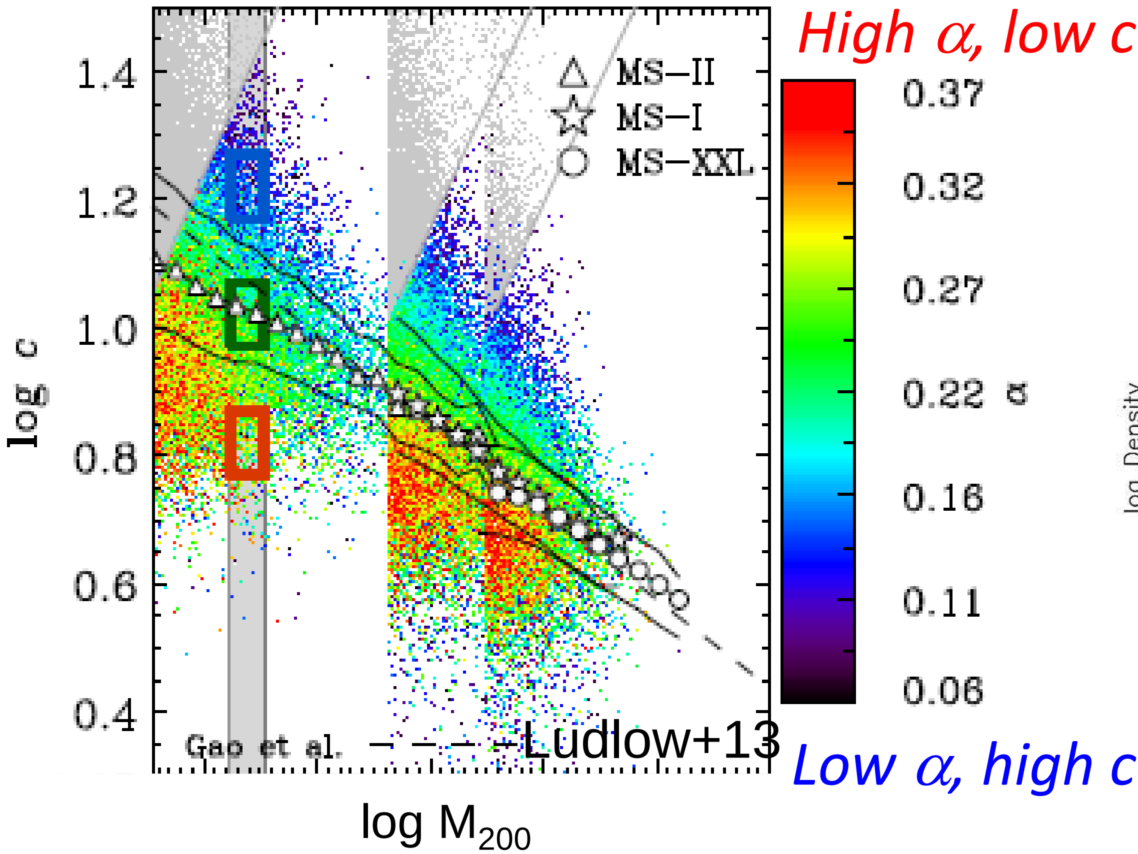

α: degree of curvature

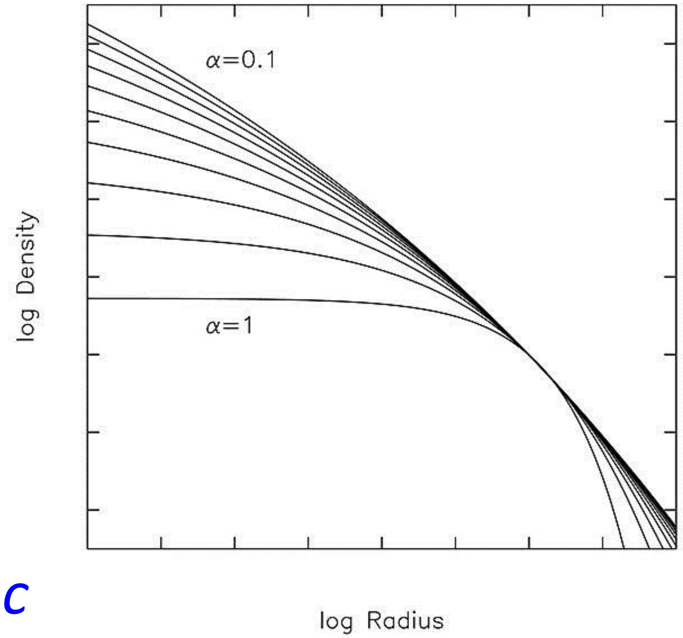

- Scatter is due to another DoF (α), related to MAH (Ludlow+13)
- Larger values of α correspond to halos that have been assembled more rapidly than the NFW curve
- Halos with average c_{200} have the NFW-equivalent α ~0.18

Key Predictions of nonlinear structure formation models

(3) Halo bias: surrounding large-scale structure

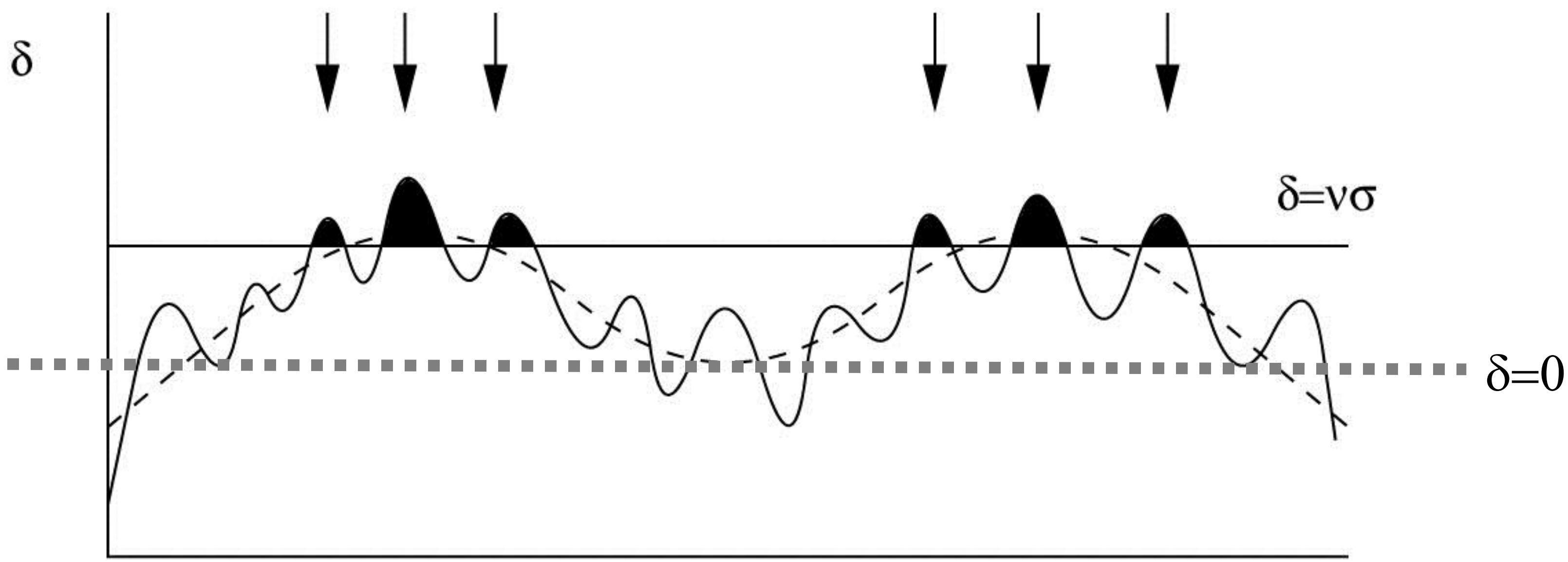

$$\delta(\mathbf{x}) := \frac{\rho - \bar{\rho}}{\bar{\rho}} = \int \frac{d^3k}{(2\pi)^3} \tilde{\delta}(\mathbf{k}) e^{i\mathbf{k}\cdot\mathbf{x}}$$

$$\left\langle \tilde{\delta}(\mathbf{k}) \tilde{\delta}(\mathbf{k}') \right\rangle = (2\pi)^3 \delta_D^3(\mathbf{k} + \mathbf{k}') P(k)$$

Halo Bias Factor: b_h

Clustering of matter around halos with *M*:

$$\xi_{hm}(r\,|\,M) \equiv \left\langle \delta_h(\mathbf{x}\,|\,M)\,\delta_m(\mathbf{x}+\mathbf{r}) \right\rangle$$

$$= \frac{\left\langle \rho_h(r\,|\,M) \right\rangle}{\bar{\rho}} + b_h(M)\,\xi_{mm}(r)$$ **2h term**

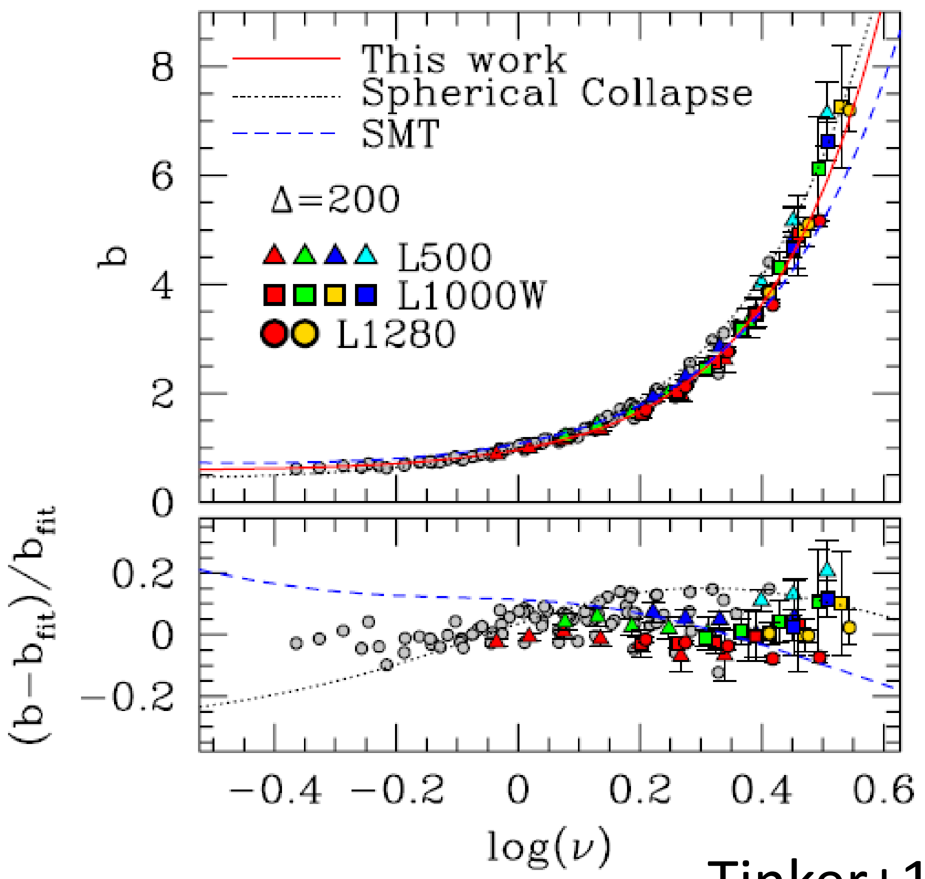

Correlated matter distribution (2h term)

Matter correlation function:

$$\xi_{mm}(\mathbf{r}) \equiv \left\langle \delta_m(\mathbf{x})\,\delta_m(\mathbf{x}+\mathbf{r}) \right\rangle = \int \frac{d^3k}{(2\pi)^3} P(k)\, e^{i\mathbf{k}\cdot\mathbf{r}}$$

$$\propto \sigma_8^2$$

Linear halo bias:

$$b_h(\nu) \approx 1 + \frac{\nu^2 - 1}{\delta_c}$$

$$\nu \equiv \frac{\delta_c}{\sigma(M,z)} \sim 3-4 \text{ for clusters}$$

Tinker+10 LCDM simulations

Non-local substructure effect

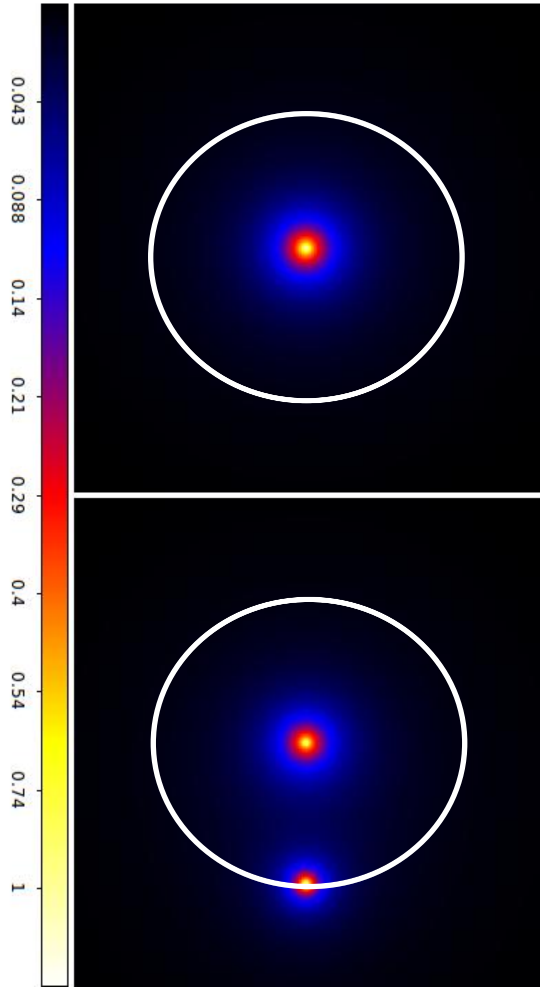

A substructure at $R \sim r_{\mathrm{vir}}$ of the main halo, modulating $\Delta\Sigma(R) = \Sigma(< R) - \Sigma(R)$

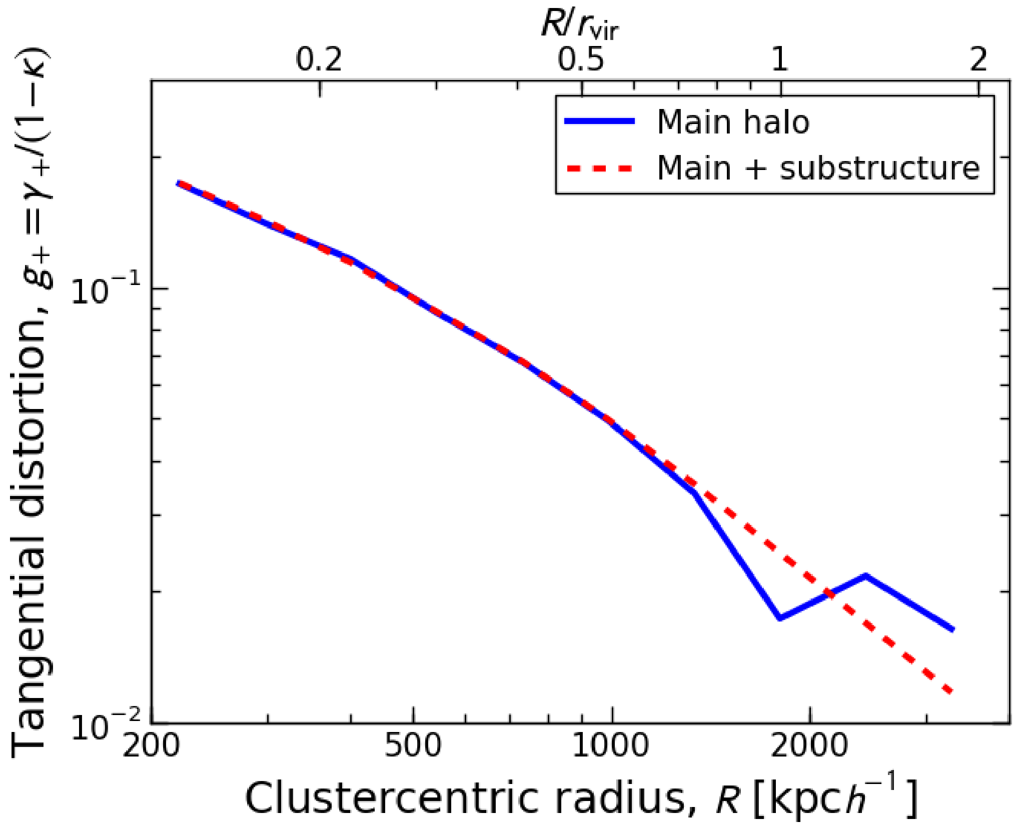

Known 5%-10% negative bias in mass estimates from tangential-shear fitting, inherent to rich substrucure in outskirts (Rasia+12)

Magnification bias effects

Flux-limited source counts:

$$n_{\rm obs}(>f) = \mu^{-1} n(>\mu^{-1} f)$$

Broadhurst, Taylor & Peacock 1995

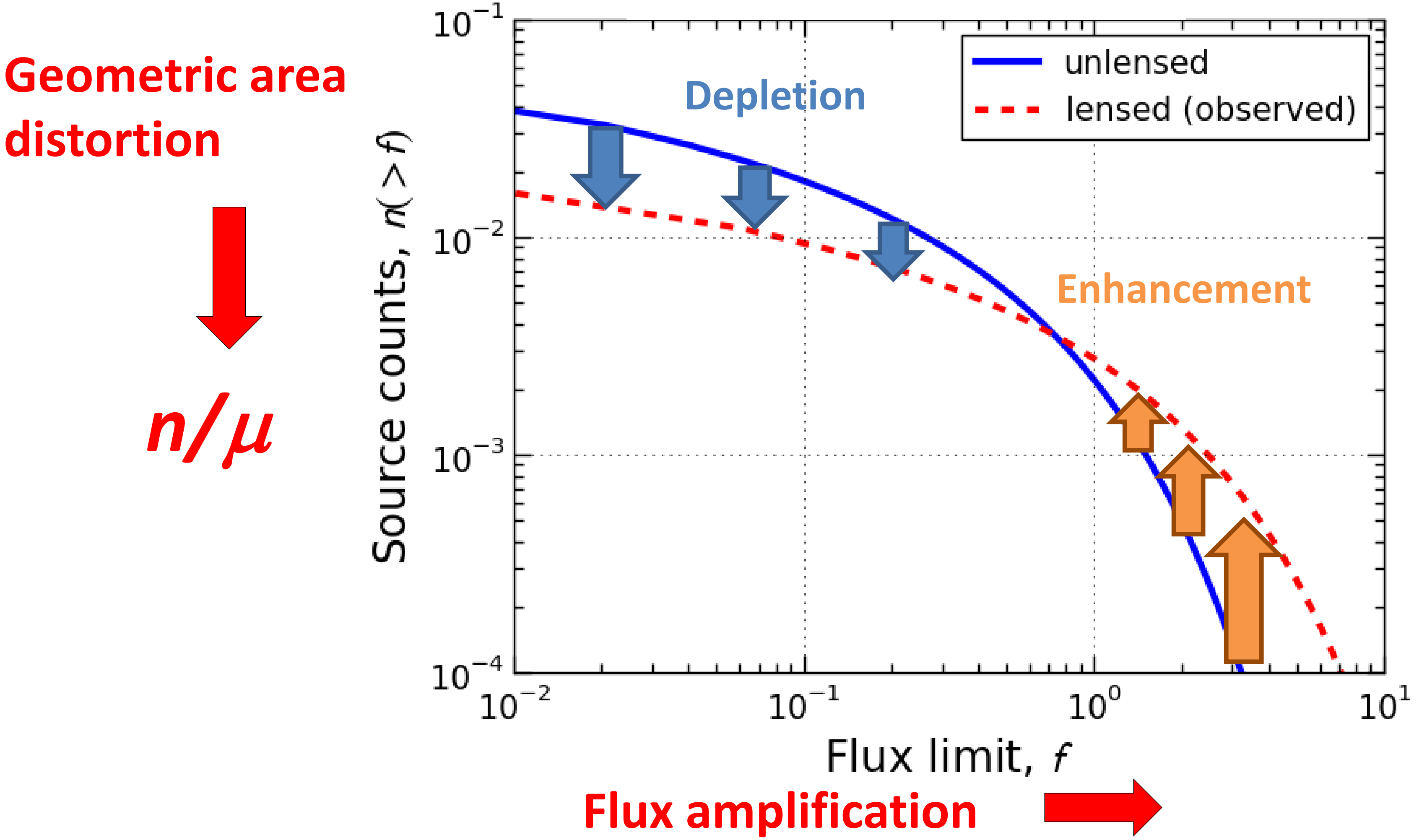

Averaged Halo Density Profile $\Sigma(R)$

Stacking lensing signals of individual clusters by

$$\langle\langle \mathbf{\Sigma} \rangle\rangle = \left(\sum_n \mathcal{W}_n \right)^{-1} \left(\sum_n \mathcal{W}_n \mathbf{\Sigma}_n \right),$$

Summing over clusters (n=1, 2, ..)

with individual "sensitivity" matrix

$$(\mathcal{W}_n)_{ij} \equiv \Sigma^{-2}_{(\mathrm{c},\infty)n} \left(C_n^{-1} \right)_{ij},$$

defined with total covariance matrix

$$C = C^{\mathrm{stat}} + C^{\mathrm{sys}} + C^{\mathrm{lss}} + C^{\mathrm{int}},$$

With "trace-approximation", averaging (stacking) is interpreted as

$$\langle\langle M_\Delta \rangle\rangle = \frac{\sum_n \mathrm{tr}(\mathcal{W}_n)\, M_{\Delta,n}}{\sum_n \mathrm{tr}(\mathcal{W}_n)}$$

Umetsu et al. 2014, *ApJ*, 795, 163

Shear doesn't see mass sheet

Averaged lensing profiles in/around LCDM halos (Oguri & Hamana 11)

Total

$$\kappa = \Sigma(R) / \Sigma_c$$

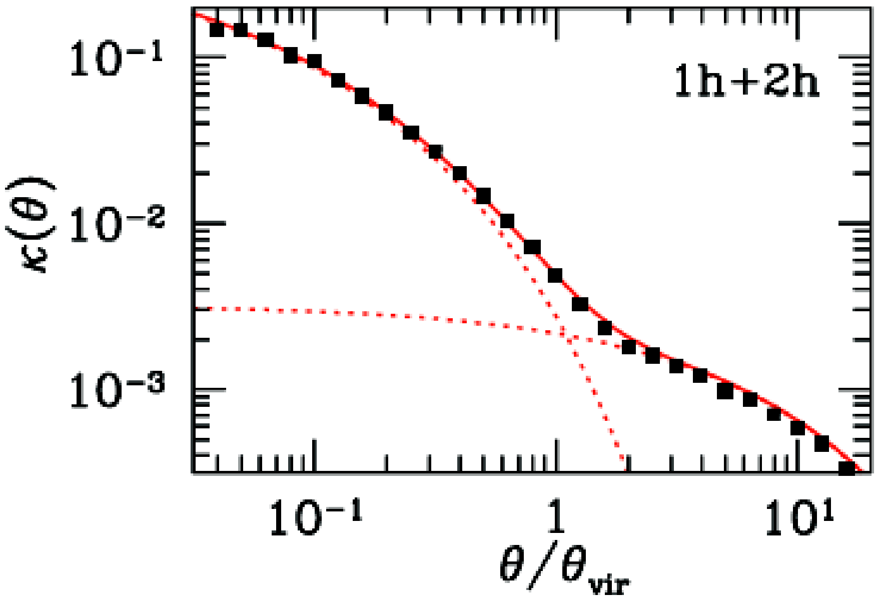

Modulated

$$\gamma_+ = \Delta\Sigma(R) / \Sigma_c$$

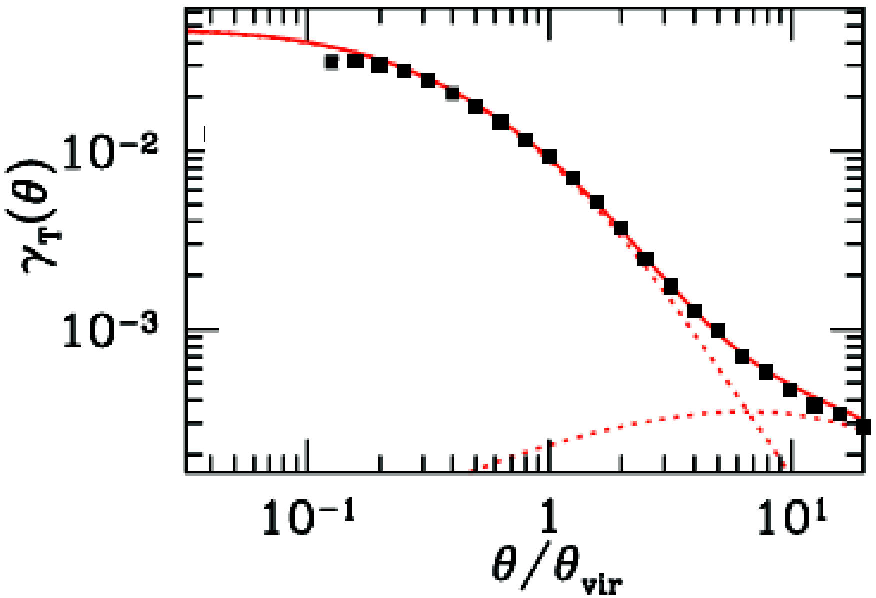

- **Tangential shear is a powerful probe of 1-halo term, or intra-halo structure.**
- **Shear alone cannot recover absolute mass, known as *mass-sheet degeneracy:***

γ remains unchanged by $\kappa \to \kappa + \text{const.}$

Concentration—Mass Relation of the CLASH X-ray-selected Subsample

Umetsu et al. 2016, arXiv:1507.04385

Concentration—Mass Scaling Relation

Consider a power-law scaling relation of the form:

$$c_{200c} = 10^{\alpha} \left(\frac{M_{200c}}{M_{piv}} \right)^{\beta} \left(\frac{1+z}{1+z_{piv}} \right)^{\gamma},$$

with pivot mass and redshift $M_{piv} = 10^{15} M_{sun}/h,\ z_{piv} = 0.34$

Define new independent (*X*) and dependent (*Y*) variables:

$$Y \equiv \log_{10} \left[\left(\frac{1+z}{1+z_{piv}} \right)^{-\gamma} c_{200c} \right],$$

$$X \equiv \log_{10} \left(M_{200c}/M_{piv} \right).$$

$$Y(X) = \alpha + \beta X$$

Redshift slope γ is fixed to the theoretical prediction for the CLASH sample, γ=-0.668 (Meneghetti+14)

Bayesian Regression Analysis

We take into account

- Covariance between observed *M* and *c*
- Intrinsic scatter in *c*
- Non-uniformity in mass probability distribution *P*(log*M*)

Conditional probability *P*(*y*|*x*) with (*x*,*y*) = observed (*X*,*Y*)

$$\ln \mathcal{P}(\boldsymbol{y}|\boldsymbol{x}) = -\frac{1}{2}\sum_n \left[\ln\left(2\pi\sigma_n^2\right) + \left(\frac{y_n - \langle y_n|x_n\rangle}{\sigma_n}\right)^2\right], \tag{35}$$

where $\langle y_n|x_n\rangle$ and $\sigma_n^2 \equiv \mathrm{Var}(y_n|x_n)$ are the conditional mean and variance of y_n given x_n, respectively:

$$\langle y_n|x_n\rangle = \alpha + \beta\mu + \frac{\beta\tau^2 + C_{xy,n}}{\tau^2 + C_{xx,n}}(x_n - \mu),$$
$$\sigma_n^2 = \beta^2\tau^2 + \sigma_{Y|X}^2 + C_{yy,n} - \frac{(\beta\tau^2 + C_{xy,n})^2}{\tau^2 + C_{xx,n}}, \tag{36}$$

where $\sigma_{Y|X}$ is the intrinsic scatter in the Y–X relation;

Marginalized Posterior Distributions

$$c_{200\mathrm{c}} = 10^{\alpha}\left(\frac{M_{200\mathrm{c}}}{M_{\mathrm{piv}}}\right)^{\beta}\left(\frac{1+z}{1+z_{\mathrm{piv}}}\right)^{\gamma}$$

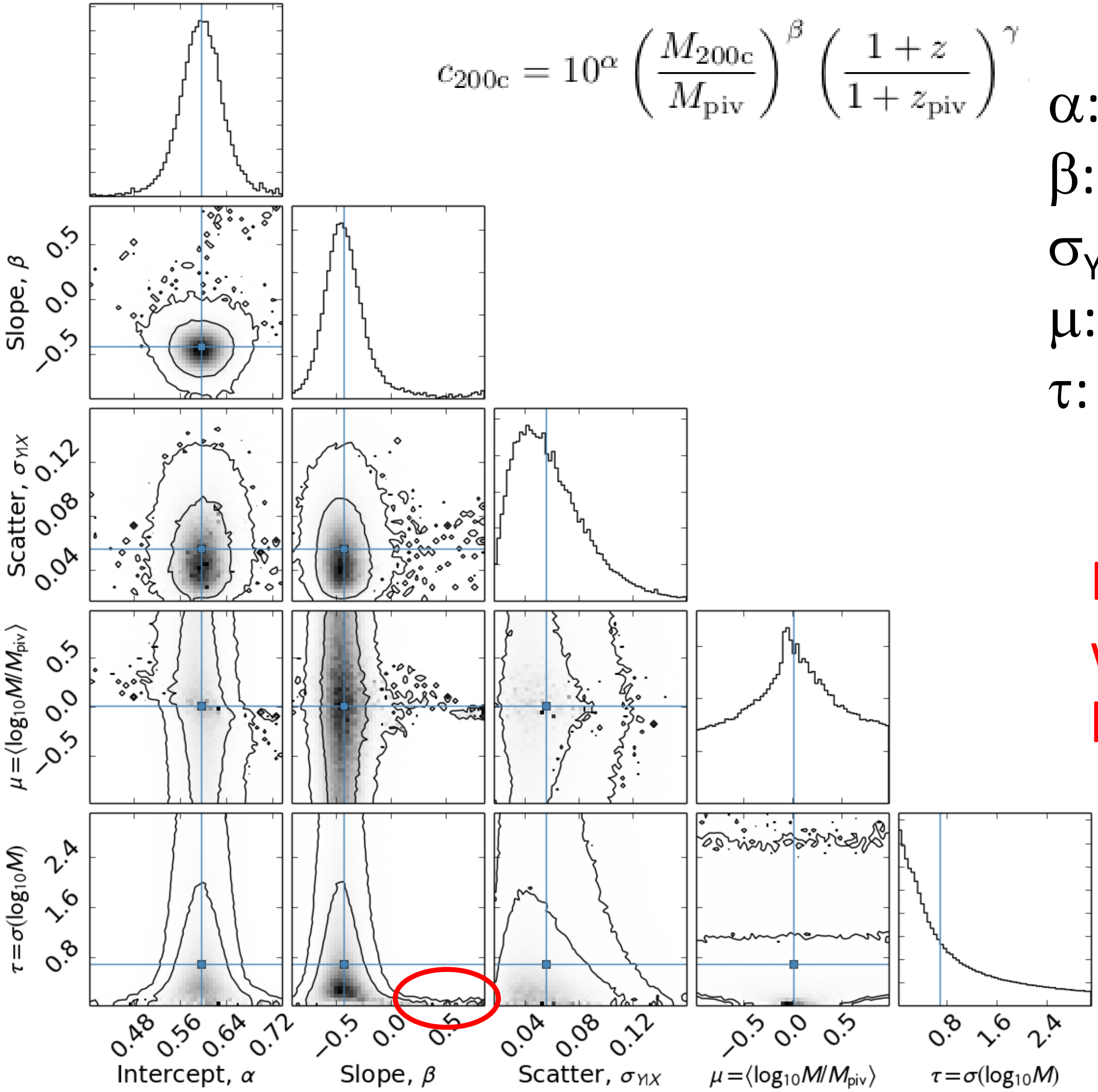

α: intercept

β: slope

$\sigma_{Y|X}$: scatter

μ: Gaussian mean of $P(\ln M)$

τ: Gaussian width of $P(\ln M)$

High β tail associated with small τ: i.e., localized $P(\ln M)$

Einasto Shape Parameter vs. Halo Mass

α_E: degree of curvature of the Einasto density profile

$$\frac{d\ln\rho(r)}{d\ln r} = -2\left(\frac{r}{r_{-2}}\right)^{\alpha_E}$$

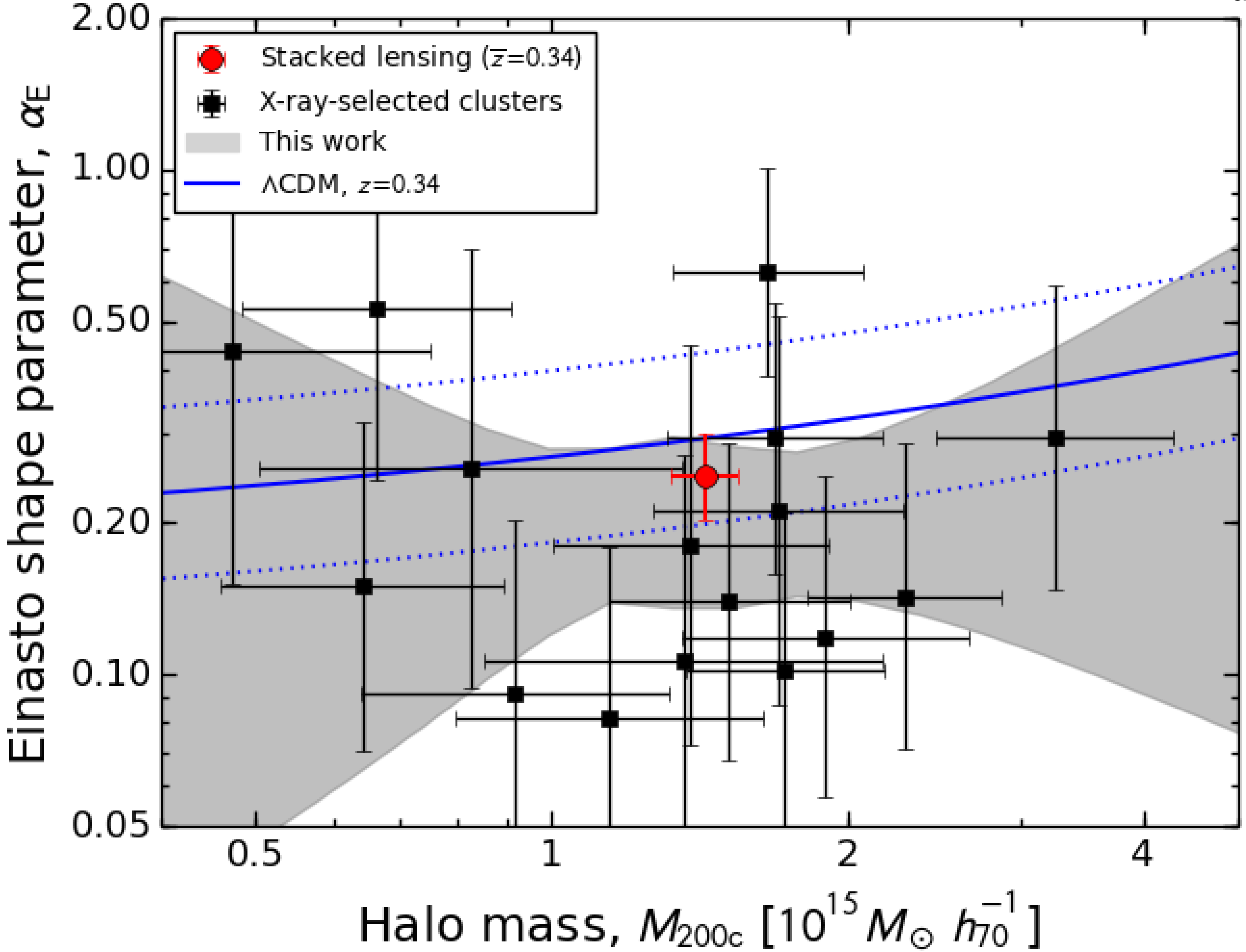

$$\alpha_E \approx 0.155 + 0.0095\nu^2 \text{ (Gao + 08)}$$

$$\nu = \frac{\delta_c}{\sigma(M)}$$

Preliminary results

Einasto Shape Parameter vs. Halo Mass

α_E: degree of curvature of the Einasto density profile

$$\frac{d \ln \rho(r)}{d \ln r} = -2\left(\frac{r}{r_{-2}}\right)^{\alpha_E}$$

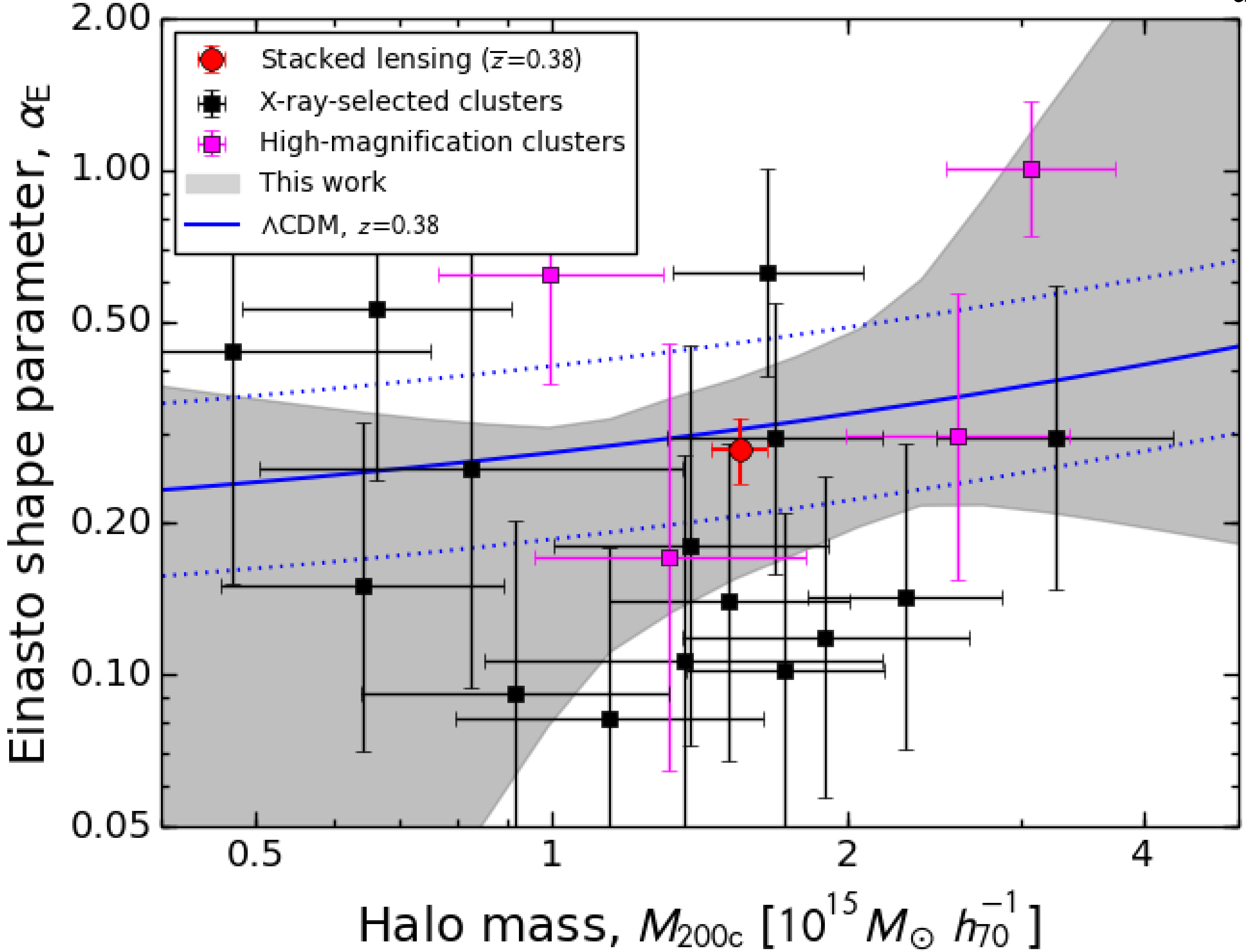

$$\alpha_E \approx 0.155 + 0.0095\nu^2 \text{ (Gao + 08)}$$

$$\nu = \frac{\delta_c}{\sigma(M)}$$

Preliminary results

Einasto Shape Parameter vs. Halo Peak Height

α_E: degree of curvature of the Einasto density profile

$$\frac{d\ln\rho(r)}{d\ln r} = -2\left(\frac{r}{r_{-2}}\right)^{\alpha_E}$$

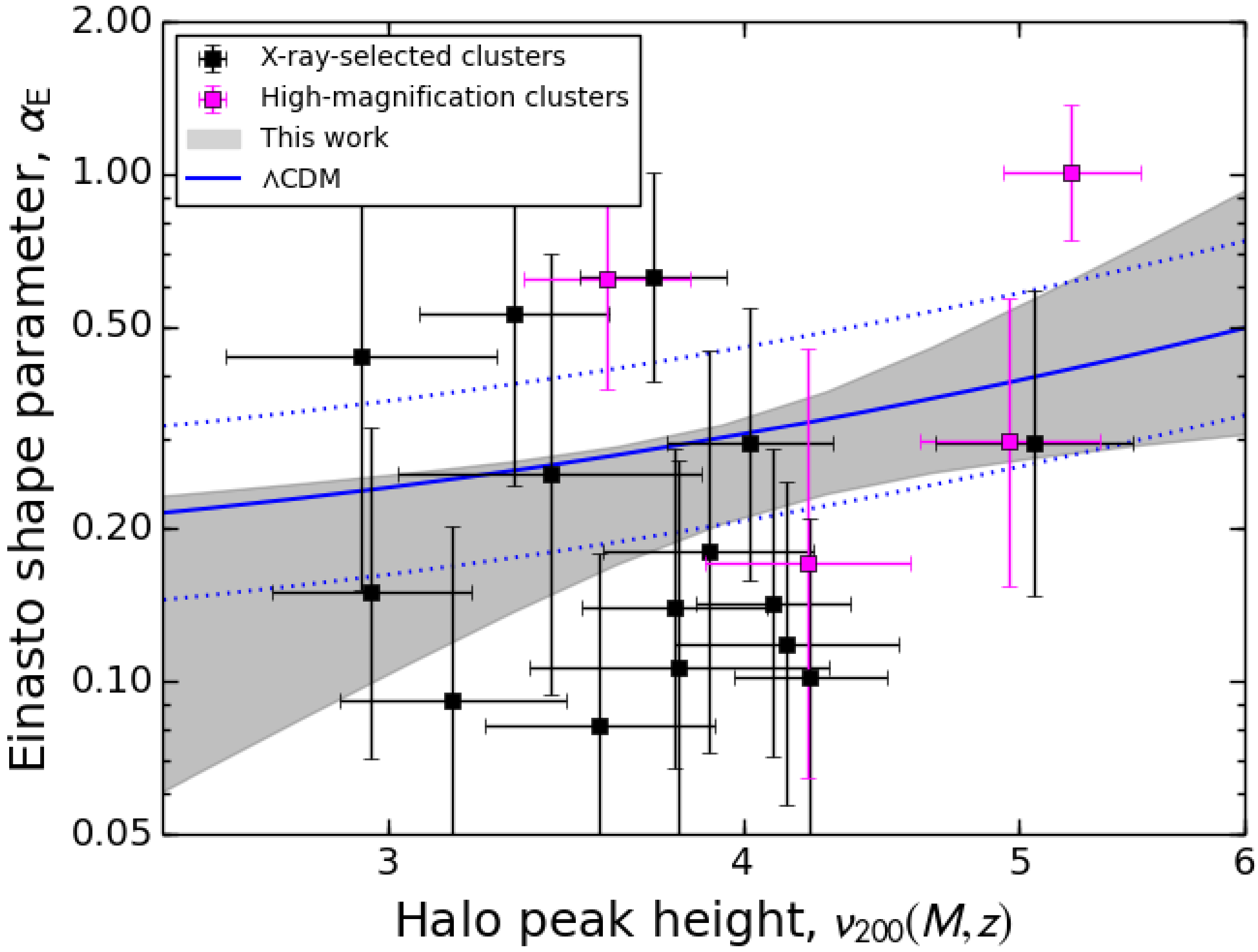

$$\alpha_E \approx 0.155 + 0.0095\nu^2 \text{ (Gao + 08)}$$

$$\nu = \frac{\delta_c}{\sigma(M)}$$

Preliminary results

CLASH *HST* Lensing Dataset

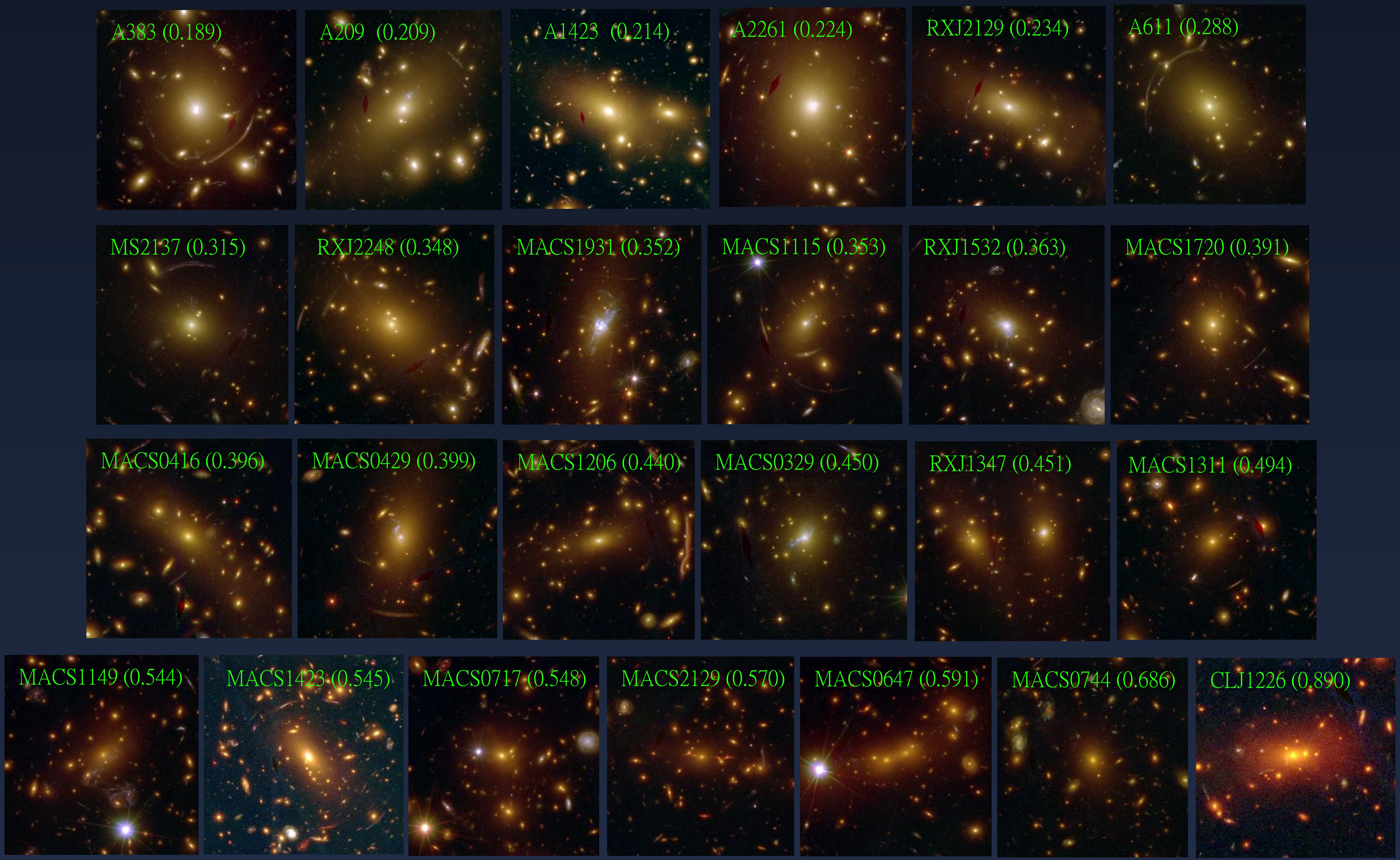

Zitrin et al. 2015, *ApJ*, 801, 44

Cluster Gravitational Lensing

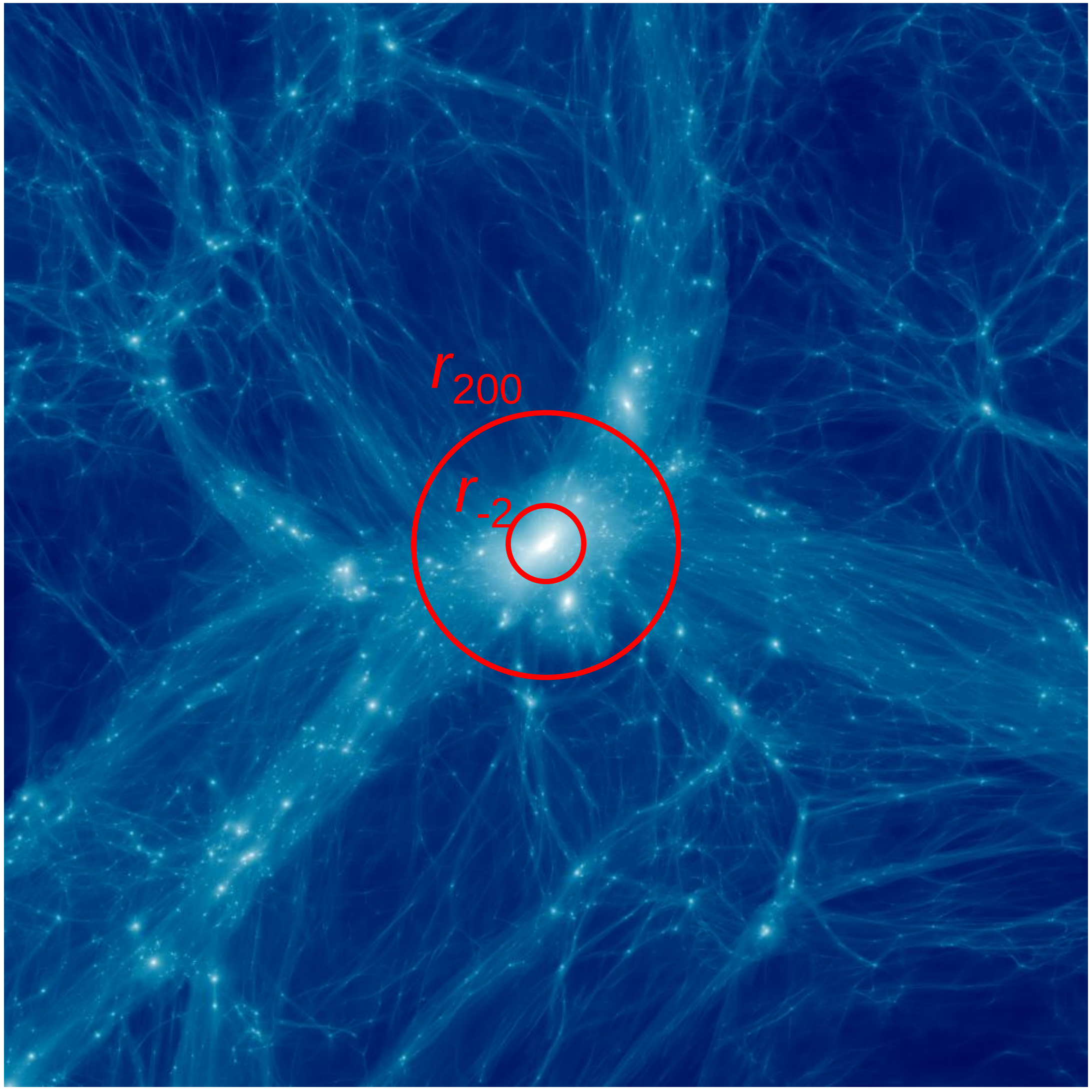

Diemer & Mansfield

Key Objectives

Intra-halo structure

Density profile, $\rho(r)$
Halo mass, M_Δ
Concentration, $c = r_\Delta / r_{-2}$
Halo asphericity

Surrounding LSS

Halo bias $b_\mathrm{h}(M)$
DM clustering strength σ_8
Assembly bias

Cluster Gravitational Lensing

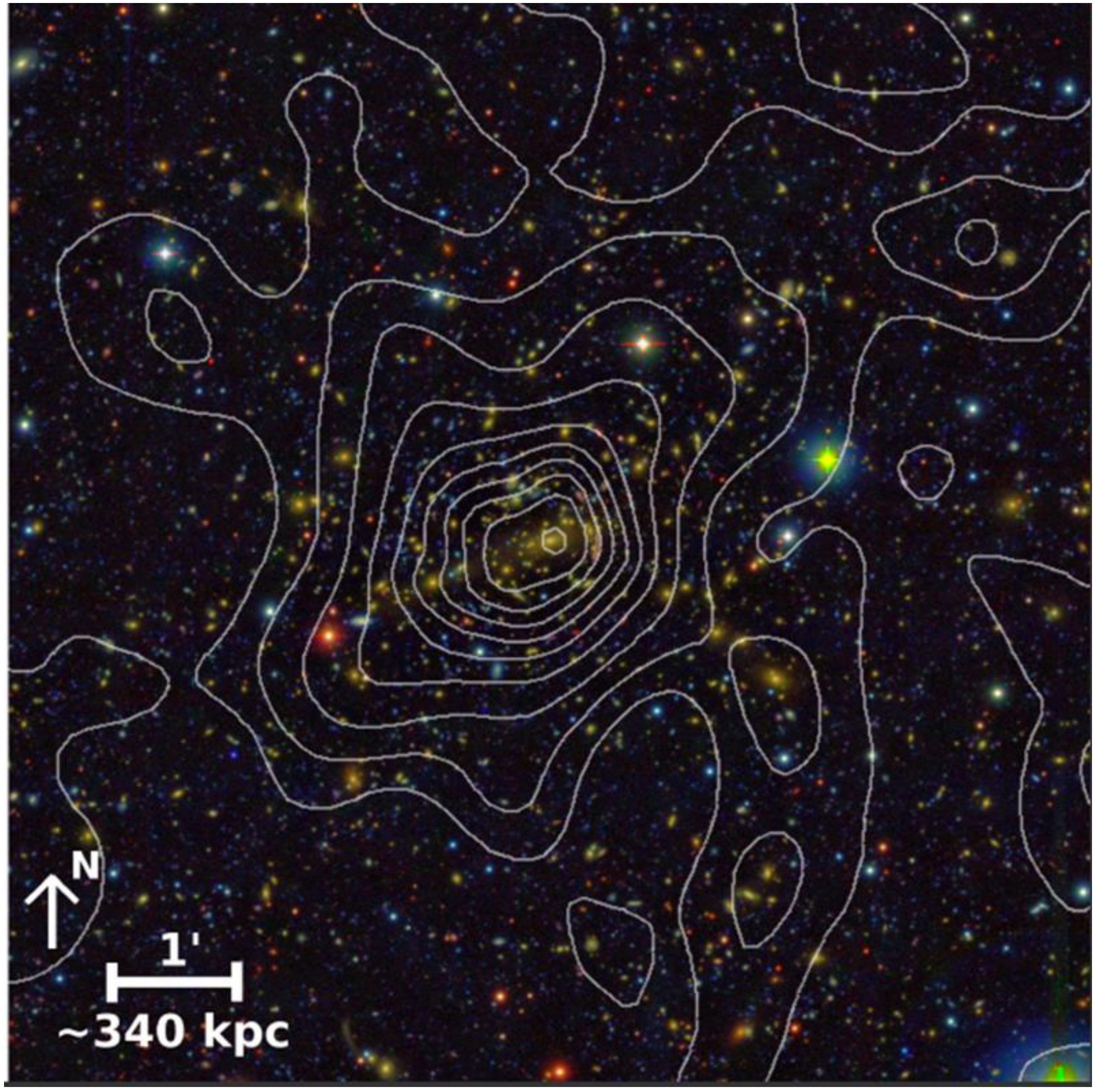

Diemer & Mansfield

Key Objectives

Intra-halo structure

Density profile, $\rho(r)$
Halo mass, M_{Δ}
Concentration, $c = r_{\Delta}/r_{-2}$
Halo asphericity

Surrounding LSS

Halo bias $b_{\rm h}(M)$
DM clustering strength σ_8
Assembly bias